

ABSTRACT

Title of Document: ENZYMATIC ACTIVITY PRESERVATION
THROUGH ENTRAPMENT WITHIN
DEGRADABLE HYDROGEL NETWORKS

Angela Marie Mariani, PhD, 2012

Directed By: Professor Peter Kofinas, Fischell Department of
Bioengineering

This dissertation aimed to design and develop a “biogel;” a reproducible, abiotic, and biocompatible polymer hydrogel matrix, that prolongs enzymatic stability allowing for rapid production of biomolecules. The researched entrapment method preserves enzyme activity within an amicable environment while resisting activity reduction in the presence of increased pH environmental challenges. These biogels can be used in a number of applications including repeated production of small molecules and in biosensors. Five main objectives were accomplished: 1) Biogels capable of maintaining enzymatic functionality post-entrapment procedures were fabricated; 2) Biogel activity dependence on crosslinker type and crosslink density was determined; 3) Biogel composition effects on sustained activity after storage were compared; 4) Biogel activity dependence on charged monomer moieties was evaluated, and 5) Combined optimization knowledge gained from the first four objectives was utilized to determine the protection of enzymes within hydrogels when challenged with an

increased pH above 8. Biogels were fabricated by entrapping β -galactosidase (lactase) enzyme within acrylamide (ACR) gels crosslinked with poly(ethylene glycol) diacrylate (PEGDA, degradable through hydrolysis) or *N,N'*-methylenebisacrylamide (BIS, non-degradable). Initial hydrogel entrapment reduced activity to 40% in ACR/PEGDA gels, compared to a 75% reduction in initial activity of ACR/BIS biogels. Once entrapped, these enzymes resist activity reduction in the presence of environmental challenges, such as altering the pH from 7 to above 8. When biogels were challenged at a pH of 8, activity retention positively correlated to PEGDA crosslinker density; increasing from 48% to 91% retention in 30 to 40 mole % PEGDA biogels as compared to solution based control which retained only 23%. Retention of activity when perturbed from pH 7 is advantageous for biogel applications including the repeated production of desired small molecules and biosensors. Biogels with positive or negative monomer moiety functionalities were also investigated to increase enzyme-matrix interactions and enzyme stability. The researched entrapment method illustrates the potential to sterically hinder and diffusively impede enzymes from performing their function, potentially enabling the reactivation of the enzyme at a site and time dictated by the user by degrading the crosslinks of the network.

ENZYMATIC ACTIVITY PRESERVATION THROUGH ENTRAPMENT
WITHIN DEGRADABLE HYDROGEL NETWORKS

By

Angela Marie Mariani

Dissertation submitted to the Faculty of the Graduate School of the
University of Maryland, College Park, in partial fulfillment
of the requirements for the degree of
Doctor of Philosophy
2012

Advisory Committee:
Professor Peter Kofinas, Chair
Professor William Bentley
Professor Robert M. Briber
Professor Mohamad Al-Sheikhly
Associate Professor Isabel K. Lloyd

© Copyright by
Angela Marie Mariani
2012

Table of Contents

Table of Contents	ii
List of Tables	iv
List of Figures	v
Chapter 1: Introduction	1
1.1 Objectives	1
1.2 Background	2
1.2.1 Problem Statement	2
1.2.2 Enzyme Functions and Kinetics	3
1.2.3 Small Molecule Synthesis: Solution Based	4
1.2.4 Enzymatic Stabalization	6
1.2.5 Enzymatic Stabilization: Polymers and Immobilization Techniques	6
1.3 Entrapment Method	8
Chapter 2: Synthesis and Characterization of Hydrogels	12
2.1 Objectives	12
2.2 Introduction	12
2.3 Methods	13
2.3.1 Materials	13
2.3.2 Synthesis of Hydrogels	13
2.3.3 Swelling	15
2.3.4 Degradation	16
2.3.5 Dynamic Mechanical Analysis	16
2.4 Results	17
2.4.1 Swelling	17
2.4.2 Degradation	24
2.4.3 Dynamic Mechanical Analysis	35
2.5 Conclusions	40
Chapter 3: Biogel Characterization at Different Crosslink Densities	42
3.1 Objectives	42
3.2 Introduction	43
3.3 Methods	44
3.3.1 Materials	44
3.3.2 Confocal Microscopy	45
3.3.3 Positive Control Studies	46
3.3.4 Enzyme Activity	49
3.4 Results	50
3.4.1 Confocal Microscopy	50
3.4.2 Positive Control Studies	53

3.4.3 Enzyme Activity	59
3.5 Conclusions	66
Chapter 4: Biogel Characterization with Positive and Negative Monomer Moieties	67
4.1 Objectives	67
4.2 Introduction	67
4.3 Methods	67
4.3.1 Materials.....	67
4.3.2 Positive Control Studies	68
4.3.3 Enzyme Activity	69
4.4 Results	70
4.4.1 Positive Control Studies	70
4.4.2 Enzyme Activity	71
4.5 Conclusions	75
Chapter 5: Overall Conclusions and Future Directions.....	76
5.1 Synthesis and Characterization of Hydrogels.....	76
5.2 Biogel Characterization at Different Crosslink Densities	78
5.3 Biogel Characterization with Positive and Negative Monomer Moieties	78
5.4 Future Directions	79
List of Acronyms	81
Glossary	82
Bibliography	83

List of Tables

Table 1: Monomers and Crosslinkers for use in Biogel Complex Optimization	15
Table 2: Calculated Fickian Swelling Constant, K_s	20
Table 3: Mechanical Properties as Determined through DMA	36
Table 4: LEM of 10% Crosslinked 0-30 % AMPS (-) Monomer	38
Table 5: SHM of 10% Crosslinked 0-30 mole % AMPS (-) Monomer	38
Table 6: LEM of 5% Crosslinked 15-30 mole % MAPTAC (+) Monomer	39
Table 7: SHM of 5% Crosslinked 15-30 mole % MAPTAC (+) Monomer	40
Table 8: V_{\max} retention of PEGDA crosslinked biogels when exposed to NaOH	66
Table 9: V_{\max} retention of biogels challenged with NaOH	74
Table 10: V_{\max} retention of biogels challenged with BBS	75

List of Figures

Figure 1. Entrapment Schematic	9
Figure 2. Entrapment and Activation Schematic.....	10
Figure 3. Swelling Behavior of BIS vs. PEGDA Crosslinked Hydrogels.....	20
Figure 4. Swelling Behavior of Charged Hydrogels Crosslinked with PEGDA.....	23
Figure 5. Degradation Behavior of BIS vs. PEGDA Crosslinked Hydrogels	27
Figure 6. Degradation Behavior of Positively Charged Hydrogels.....	30
Figure 7. Degradation Behavior of Negatively Charged Hydrogels	33
Figure 8. Stress vs. Strain DMA Results in Various States of Swelling.	37
Figure 9. Confocal Imaging of Entrapped Enzyme.....	51
Figure 10. Lineweaver-Burke plots of Enzyme Diffusion	56
Figure 11. Lineweaver-Burke plot of Alginate Entrapment of Enzyme	58
Figure 12. Alginate Fabrication and Dissolution in PBS	58
Figure 13. Alginate Biogels Converting ONPG into ONP.....	59
Figure 14. Lineweaver-Burke plot: Experimental Setup and Analysis.....	61
Figure 15. V_{\max} over a Two Day Period: Low Crosslink Density Studies.....	62
Figure 16. V_{\max} over a Two Day Period: High Crosslink Density Studies	64
Figure 17. Calculated K_m over all Studies.....	65
Figure 18. Calculated V_{\max} Two Day Study: Charged Matrices	72

Chapter 1: Introduction

1.1 Objectives

The aims of this dissertation were to prolong enzymatic stability allowing for rapid production of biomolecules. This was completed by designing and developing a reproducible, abiotic, and biocompatible enzyme polymer hydrogel matrix, hereafter referred to as “biogel.” Biogels entrap specific enzymatic proteins to take advantage of biologically natural small molecules production. Five main objectives were developed to accomplish this aim. The first objective was to fabricate enzymatically active hydrogels, “biogels,” capable of maintaining the functionality of enzymes post-entrapment procedures. β -galactosidase (lactase) enzyme was entrapped within hydrogel matrices of acrylamide (ACR) crosslinked with *N,N'*-methylenebisacrylamide (BIS, non-degradable) or poly(ethylene glycol) diacrylate (PEGDA, degradable) to create active biogels. Enzyme activity was confirmed through ortho-nitrophenol (ONP) production as ortho-nitrophenyl- β -D-galactopyranoside (ONPG) substrate is catalyzed by lactase, yielding one galactosidase molecule and one ONP molecule. ONP can be easily used to report lactase activity as it readily absorbs light at $\lambda = 420$ nm. The second objective was to determine the dependence of crosslinker type and crosslink density on the enzymatic activity. Crosslinker type and density have large impacts on the mechanical and diffusive properties of hydrogels. These properties were assessed utilizing dynamic mechanical analysis (DMA), swelling and degradation studies, and confocal imaging of enzymes within the matrix. Such material parameters aid in the understanding of bulk effects

on stored enzymatic stability. The third objective was to evaluate the sustained enzymatic activity retained in the biogels after storage and the ability for biogel reuse over multiple days. Testing the enzyme kinetics over a two day study yields information allowing for optimization of the biogel for applications requiring storage and reuse of enzymes for the production or degradation of small molecules. The fourth objective was to compare the enzyme activity dependence on charged monomer synthesis moieties. Charged hydrogel matrix monomers can affect the enzyme pocket within the polymer matrix, allowing for electrostatic interactions between the matrix and the protein, aiding in the stabilization of the enzyme's tertiary structure. The fifth objective was to use the combined optimization knowledge gained from the first four objectives to determine the protection of enzymes within the biogels when challenged with an increased pH of 8. At this pH, enzyme will denature and the PEGDA crosslinker will begin to degrade, creating larger pockets for the enzyme. Increasing protection during this type of environmental test shows the potential to use these biogels for on-demand applications requiring the degradation of crosslinks for the re-animation of the entrapped enzyme.

1.2 Background

1.2.1 Problem Statement

The ultimate aim of this project was to prolong enzymatic stability allowing for the reliable, sustained, and repeatable production of desired small biomolecules. The entrapment method preserves enzyme activity within an amicable environment to resist activity reduction in the presence of increased pH environmental challenges.

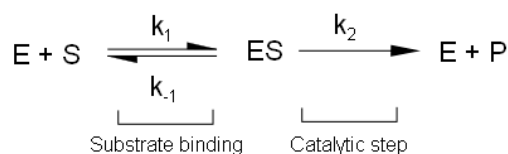
These biogels can be used in a number of applications including the repeated production of desired small molecules and potential use in biosensors. Depending on the application, the ability to activate the biogel from a dormant state to a catalytically active state would be a huge advantage over current methods. This would allow for enzymatic protection in a dormant state and activation on-demand at a site and time dictated by the user. Specifically, one application of this work may be used in the production of small cell signaling molecules, which are otherwise difficult to produce and/or purify, as well as in the degradation of small molecular toxins and other environmental hazards.

1.2.2 Enzyme Functions and Kinetics

Typical biomolecule formation is directed through multiple protein enzymatic reactions in site-specific cellular structures such as organelles (1-3). Generally, signal peptides direct the compartmentalization of the necessary enzymatic proteins for biomolecule production. Employment of this natural grouping allows the required proteins to become organized and assembled into the desired biomolecules. This work took advantage of biomolecule production utilizing natural enzymatic processes. This was done by entrapping enzymes within abiotic hydrogel networks to investigate the synthesis of biomolecules.

Enzymes are biological catalysts, which break down specific substrate precursor molecules into desired product molecules to be utilized by cells. Each enzyme is made up of a long chain of specific amino acids which, when folded, create an active three-dimensional protein. These enzymatic proteins have one or more active sites where interactions with the substrate occur. Heat, pH variance, or

chemical denaturants can cause the unfolding or partial unfolding of these proteins yielding denatured and inactivated amino acid chains. Enzymes [E] increase the general transference coefficient and act as chemical catalysts by greatly reducing the effective activation energy (E_a) of the reactants to prefer the molecular structure of product molecules (4, 5). The decrease of E_a is primarily responsible for enzyme-substrate activity as described by the lock and key model. This model is used to explain enzymatic binding of a specific substrate, [S], which lowers the effective E_a of the molecule, and through a ratchet movement, chemical bonds are broken and rearranged to form product molecules [P]. These product molecules are bound with a lesser affinity to the enzyme causing them to detach, leaving the enzyme free to rebind a new substrate molecule to begin the process again (6, 7).



The lifetime of enzymes depends on the overall stability of the protein in the given environment. Many factors including temperature, pH, presence of oxidizing molecules and surfactants, affect the conformational stability of enzyme. Much research has been conducted to improve enzyme stability and longevity in order to increase the small biomolecule production and degradation in non-ideal enzymatic protein environments (8-13).

1.2.3 Small Molecule Synthesis: Solution Based

Some current methods, *in-vitro*, *in-vivo* and chemical, have been used to actively produce desired small biomolecules (14-16). *In vitro* synthesis typically requires the

amplification of genes to produce large quantities of the required enzymes. These enzymes are then extracted from the bacteria through digestion of the cells and purification. The next steps require the addition of substrate for product molecule production. The product must then be purified through size-fractioning to rid the solution of the enzyme and the majority of small chemical byproducts (17). This method is costly and time consuming, often leading to low-yield product. Similar to *in vitro* synthesis methods, the techniques of *in vivo* synthesis utilizes animal models to biologically manufacture the desired product. In this method, additional small molecules are present with the desired biomolecules due to the whole organism manufacturing mechanisms. These additional byproducts greatly add to the complexity of the purification process (14).

Further, the chemical synthesis biomolecules typically utilize many volatiles and is inefficient at removing chemical reactants. Even after purification and evaporation, trace amounts of reactants are present (15). Chemical synthesis and degradation of molecules include many expensive steps and often lead to hazardous byproducts. The work of Wagner *et al.* describes the harmful ecological consequences of chemical halogenation for the production of substances such as bleach and pesticides as well as the benefits of utilizing biohalogenated chemicals which are similar (in some cases identical) to their chemically synthesized counterparts (18).

1.2.4 Enzymatic Stabilization

Previously used techniques to stabilize enzymes include: genetic point alteration, chemical modification, and the addition of additives such as glycerol and sugars (8, 11).

1.2.4.1 Genetic Point Alteration and Chemical Modification

Genetic point alteration and chemical modification methods alter the enzyme itself and can cause unnatural tertiary structures to form, leading to the destruction of the active site or substrate diffusion issues (19). For example, in gluteraldehyde fixation, immobilization is achieved by crosslinking the enzyme's peripheral lysine residues. Alonso *et al.* recorded an average loss of activity of 20% due to this immobilization process (9).

1.2.4.2 Additive Stabilization

To strengthen hydrophobic interactions between non-polar amino acids, additives such as DMSO and glycerol have been used to create rigid segments of the enzyme that resist structural degradation and solvent/enzyme interactions. These techniques have shown to increase protein longevity within a sub zero atmosphere (8, 20). Another method, such as biopolymer entrapment by alginate, is inexpensive and can be done in mild conditions. The drawbacks to this method are that it tends to have low mechanical strength and high enzyme leakage due to large pore size (21).

1.2.5 Enzymatic Stabilization: Polymers and Immobilization Techniques

1.2.5.1 Site Specific Polymer Attachment

Polymers have also been used in combination with enzyme alteration such as in the research of Marsac *et al.* This work describes the site-specific attachment of

PEG to Rab6, a vascular trafficking enzyme. Site specific polymer attachment to Rab6 caused no activity losses while improving the enzyme solubility and, similar to the discussed additives, aided in enzymatic resistance to degradation (20).

1.2.5.2 Enzymatic Adsorption onto Matrices and Use of Polymers as Additives

Bellusci *et al.* combined polymer chemistry and biological attachment of enzymes by adsorbing lipase enzyme onto ethylene-vinyl alcohol polymers functionalized with acetyl chlorides (22). In addition to these methods, synthetic polymers including PEG and polyvinyl alcohols (PVA) have been shown to increase enzyme stability by limiting solvent/enzyme interactions through non-specific polymer-enzyme interactions (8, 11).

1.2.5.3 Hydrogel Immobilization

Immobilizations by protein entrapment within various hydrogel and polymeric networks have also been shown to increase stability and lifetime of enzymes (10, 23-28). When entrapped within a hydrogel network, enzymatic protein activity highly depends upon the cavity size within the hydrogel matrix. Increased crosslink density of the matrix creates smaller hydrated pores within the network (29). Hydrogel/enzyme interactions are utilized to maintain enzymatic stability over extended time periods, during cycling, and pH excursions due to environmental effects. A denatured protein can be described as an unfolded, inactive protein. Reducing movement and protein conformational changes has shown to increase the length of activity of the enzyme (23, 25, 26, 28). Covalent bonds between enzyme and matrix may completely eradicate all normal enzymatic functional behaviors by pinning it to the matrix in an unfavorable conformation causing all activity to be lost.

Contrarily, a tight-fitting cavity of gel around the enzymatic protein, *without* covalently binding the enzyme to the gel matrix, serves to increase enzymatic life and overall small molecule conversion over multiple cycling periods. In each cycle, fresh substrate is supplied to the biogel and allowed to react until all substrate is consumed. The cycle can be repeated by removing the biogel, leaving pure product molecules in solution behind, and placing it in a fresh substrate supply to allow conversion to continue. Increased matrix/enzyme interactions will create the desired cavity while not impinging on the enzyme's natural functions (23, 28). Hydrophobic interactions are important typically in the conservation of preferential enzyme conformations since maintaining natural hydrophobic pockets within the enzyme allow the active sites to be revealed (30).

1.3 Entrapment Method

The objective of this work is to go beyond current entrapment procedures to create versatile and stable biogel reactors for enzymatic catalyzed reactions. Experiments were designed to create a library of enzymatic friendly hydrogel constructs to allow for the biogel creation of a user's choice. Figure 1 shows the basic method utilized for biogel synthesis, which incorporates the enzyme within a favorable matrix to allow for long term use and reuse of the biogel complex to catalyze a large variety of reactions.

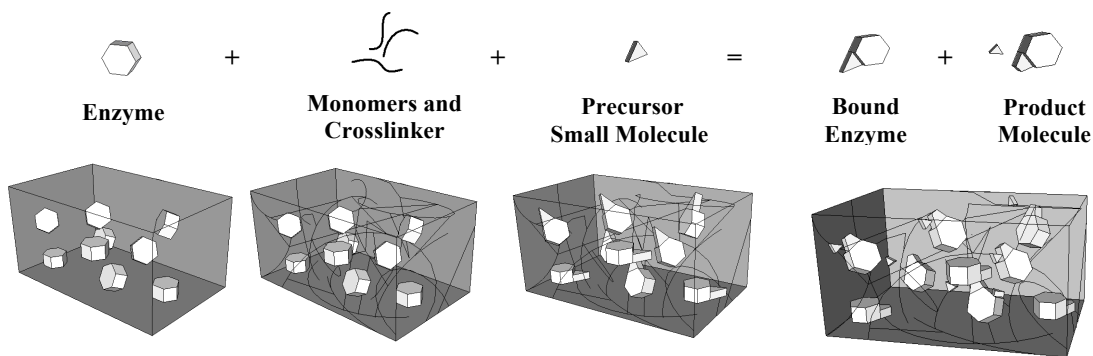


Figure 1. Entrapment Schematic

A schematic representation of the entrapment techniques used in this work. Monomer units are added to an enzyme solution, allowed to associate, and are then polymerized through free radical polymerization to stabilize the enzyme. The addition of precursor molecules leads to bound enzymes and product molecules.

The methods used in this work relied on the versatility of acrylate monomer units and crosslinkers to create biogel variability in charge density and cavity size to best stabilize the enzyme. Along with the matrix adaptability advantages of using these acrylate units, they also readily dissolve in the enzyme friendly media, phosphate buffered saline (PBS). A drawback to using these acrylate units is that they are polymerized using free radical initiation and propagation. A free radical in solution has the ability to attack enzymes and alter their conformation, effectively denaturing them. Other polymerization methods, such as using UV irradiation, also have similar denaturation effects on proteins and were therefore predetermined a necessary loss of activity (31, 32).

This technique was then evolved to incorporate a potential switch mechanism (PEGDA degradation) for biogel activation. Figure 2 describes the synthesis method in which biogels are highly crosslinked, prohibiting natural enzymatic-substrate binding and subsequent catalytic conversion of substrate into product molecules. Degradation, through hydrolysis of the internal bonds of PEGDA, potentially allows

for the on-demand initiation of the biogel reaction with precursor molecules to create the desired enzymatic catalytic reaction and products.

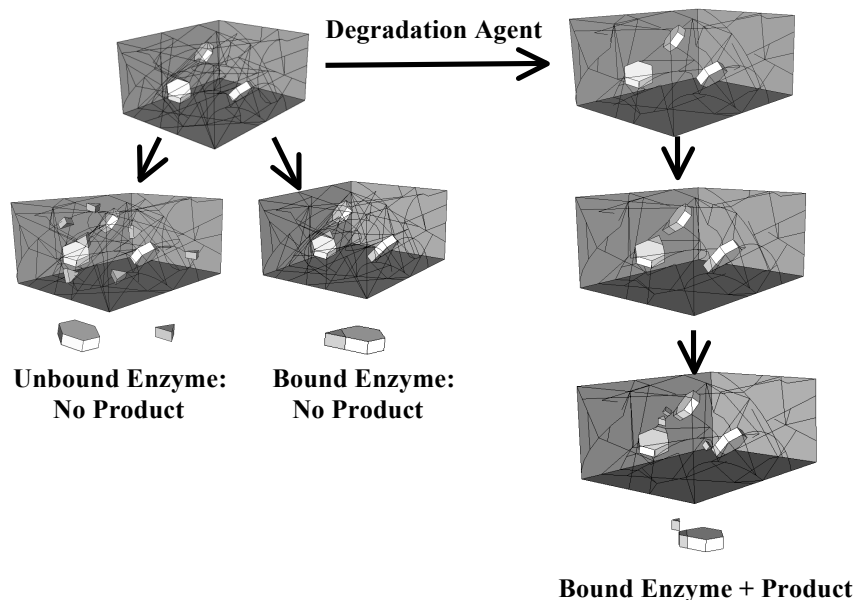


Figure 2. Entrapment and Activation Schematic

Schematic representation of entrapment procedure where enzyme is immobilized within highly crosslinked networks. Figure represents three potential enzymatic pathways dependent on degradation of the crosslinks to allow natural enzymatic function to take place. In a highly crosslinked state substrate will not bind or it will bind without the ability to become catalyzed into its product molecules. Degradation of the crosslinker allows normal enzymatic function to return to the biogel.

These hydrogels were tested for bulk properties including mechanical strength, swelling and degradation rates. Determining these parameters allows for the relation between bulk material properties to enzyme activity stability under a variety of conditions. Biogels were fabricated to test the enzymatic stability post-entrapment, reliability in repeated production cycles, and the ability of the matrices to protect the enzymatic proteins from denaturation. Charged monomers were utilized to increase the matrix/enzyme interactions and create favorable pockets for enzyme entrapment.

Enzyme kinetics were determined for synthesized biogels for use as a reliable comparative diagnostic tool to determine the stability of enzymes entrapped within matrices of different crosslink density and monomer makeup.

Chapter 2: Synthesis and Characterization of Hydrogels

2.1 Objectives

This chapter's aim is to determine hydrogel synthesis and characterization of bulk hydrogel properties to later be compared with enzymatic activity results. The four main objectives were to determine: 1) the synthesis requirements for mechanically stable hydrogels; 2) the swelling parameters of fabricated hydrogels; 3) the mechanical strength of the hydrogels, and 4) degradation kinetics of the fabricated hydrogels. Objectives 1 and 3 were completed through DMA of fabricated gels, objectives 2 and 4 were determined through mass increase investigations after swelling in PBS or 500 μ M NaOH solutions, respectively.

2.2 Introduction

To fulfill these four objectives, DMA, swelling and degradation studies were performed on fabricated hydrogels without enzyme. The mechanical properties, namely the linear elastic and strain hardening moduli, of the hydrogels were determined using DMA. Two hydrogel swelling states were tested; the “as-synthesized” state and fully swollen state. The data obtained for “as-synthesized” gels determined the original fabrication mechanical strengths and, when found to be robust, translates into ease of use for the end product consumer. Data obtained for fully swollen states related to the microstructure surrounding the enzyme during biogel fabrication of product molecules from substrate. This information was useful in relating bulk gel properties with enzyme stability and biogel recycling for multiple

production cycles. Swelling studies performed on BIS and PEGDA crosslinked hydrogels aided in the understanding of diffusive parameters that affect the maximum velocity of enzymatic substrate conversion into product in the fabricated biogels. Degradation studies of the networks led to insights involving the protection of enzymes through the use of highly crosslinked PEGDA hydrogels.

2.3 Methods

2.3.1 Materials

Acrylamide (ACR), 3-(methacryloylamino)propyl]trimethylammonium chloride (MAPTAC – positive) 2-acrylamido-2-methyl-1-propanesulfonic acid sodium (AMPS - negative), *N,N'*-methylenebisacrylamide (BIS), poly(ethylene glycol)diacrylate (PEGDA, Mn=700), ammonium persulfate (APS), and *N,N,N',N'*-tetramethylethylenediamine (TEMED), were purchased from Sigma Aldrich and were used as received except for MAPTAC and PEGDA which were first filtered through an inhibitor removal column prior to application. A dynamic mechanical analysis (TA Instrument Q800, DMA) was used in submersion compression mode to obtain linear elastic modulus of gel compositions.

2.3.2 Synthesis of Hydrogels

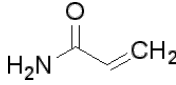
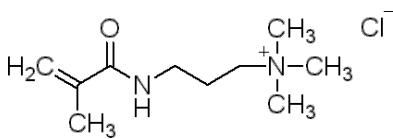
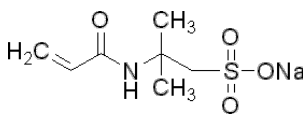
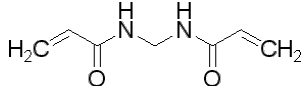
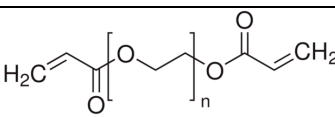
The abiotic polymer gels synthesized were compositions of the monomers and crosslinking agents shown in Table 1. Fabrications focused on: 1) hydrogel cavity size, which was altered by varying crosslinker type and crosslink densities within the polymer matrix, and 2) how the internal charge density of the hydrogel affected the

mechanical properties, which were determined through the addition of positively and negatively charged monomer moieties within the gel.

To best stabilize the enzyme, this work relied on the versatility of acrylic/acrylate monomer units and crosslinkers allowing for biogel variability of charge density and cavity size. These reagents readily dissolve in phosphate buffered saline (PBS). Polymerization of acrylic/acrylate units is through free radical initiation and propagation. Free radicals in solution can attack chemical bonds of enzymes, altering their conformation, effectively denaturing them.

The polymer hydrogels were synthesized from the polymerization of various acrylic monomers in PBS as seen in Table 1. These monomers were polymerized under an oxygen environment in the presence of various amounts of the crosslinking agent BIS or PEGDA in order to alter gel cavity size. The degradation of PEGDA is caused by hydrolysis of the internal ether groups, using an acid or a base. ACR was free radically polymerized with MAPTAC to investigate positively charged monomer/enzyme interactions; or AMPS to investigate the effects of negatively charged monomer/enzyme interactions. The hydrogel networks were initiated through the use of free radicals from APS stabilized by TEMED. The positively charged monomer, MAPTAC, and biodegradable crosslinker, PEGDA, used for these studies is stabilized with monomethyl ether hydroquinone (MEHQ). To help negate the effects of MEHQ on the hydrogel polymerization process, these monomers were run through an MEHQ removal column before being polymerized in the biogel systems.

Table 1: Monomers and Crosslinkers for use in Biogel Complex Optimization

Acrylamide (ACR)	
[3-(methacryloylamino) propyl] trimethylammonium chloride (MAPTAC) (positive)	
2-acrylamido-2-methyl-1-propanesulfonic acid sodium (AMPS) (negative)	
<i>N,N'</i> -methylenebisacrylamide (BIS) (non-degradable crosslinker)	
Poly(ethylene glycol) diacrylate (PEGDA) (degradable crosslinker)	

Images obtained from supplier: Sigma Aldrich.

Hydrogels were formed with the desired crosslinker type, crosslink density and monomer moiety amount in bitac lined 24 well plates. Three 500 μ L gels of each type were fabricated for the studies to follow. ACR will grow linearly in aqueous polymer solution containing only ACR monomer and free radicals, whereas hydrogels are formed through crosslinking these lengths of linear ACR together forming a hydrogel mesh.

2.3.3 Swelling

Swelling studies were performed on ACR gels with 1, 5, 10, 13, 15 and 20 mole % crosslink density using BIS or PEGDA as crosslinkers. Three 500 μ L gels of each crosslink density were cast in 24 well plates. Gels were first dried from their synthesized state obtaining their original dry mass (M_0). Gels were then placed in 5 mL aqueous PBS for swelling studies. Measurements were taken every 20 minutes

for the first 4 hours then every hour up to 8 hours, and finally every 4 hours till the 20 hour mark.

2.3.4 Degradation

Degradation studies were performed on ACR gels with 1, 5, 10, 13, 15 and 20 mole % crosslink density with BIS or PEGDA as crosslinkers. Three 500 μ L gels of each crosslink density were cast in 24-well plates. Gels were first dried from their synthesized state obtaining their original dry mass (M_0). Gels were then placed in 5 mL aqueous PBS for swelling studies. Degradation studies were commenced from the maximum PBS swelling point by submerging each sample in 2 mL of a 500 μ M NaOH degradation solution. Samples were weighed daily until the gels became mechanically weak and unable to handle. The degradation solution was refreshed after each weighing.

2.3.5 Dynamic Mechanical Analysis

DMA studies were performed to determine the linear elastic and strain hardening moduli for each gel as synthesized and when fully swollen in PBS (5 hour submersion). DMA was performed in compression and submersion compression mode using a multi-strain sweep of 0-6% sample height deformations at 1 Hz. Samples were placed in a submersion compression clamp containing aqueous PBS buffer and strained between 0 and 6% or until sample failure. Linear elastic moduli were calculated from the 0 to 1% strain region and strain hardening moduli were calculated from the 4 to 5% strain region. Swelling was reported as a ratio of dry

mass as calculated in Equation 1, where M_0 is the mass of samples after drying at room temperature for 24 hours and M_t is the swollen mass at time t .

$$SR = \frac{(M_t - M_0)}{M_0} \quad (\text{Equation 1})$$

2.4 Results

2.4.1 Swelling

2.4.1.1 Crosslinker type and Crosslink Density Studies

Swelling studies were performed for 1-20 mole % BIS (non-degradable) and 1-25 mole % PEGDA (degradable through hydrolysis) crosslinked gels without enzyme and are shown in Figures 3a and 3b, respectively. Data is represented as a swelling ratio as calculated from Equation 1. Typical to Fickian swelling behavior, the first 50% of obtained experimental swelling data increased linearly indicating that the swelling reactions were controlled exclusively by the chemical potential gradient of water into the matrix. To determine swelling parameters, the swelling was assumed to be Fickian and the first 50% of experimental hydrogel swelling percentages (SP) were fitted to the following Fickian swelling relation (Equation 2) as described by Peppas et al. assuming no polymer relaxation term (22, 33, 34).

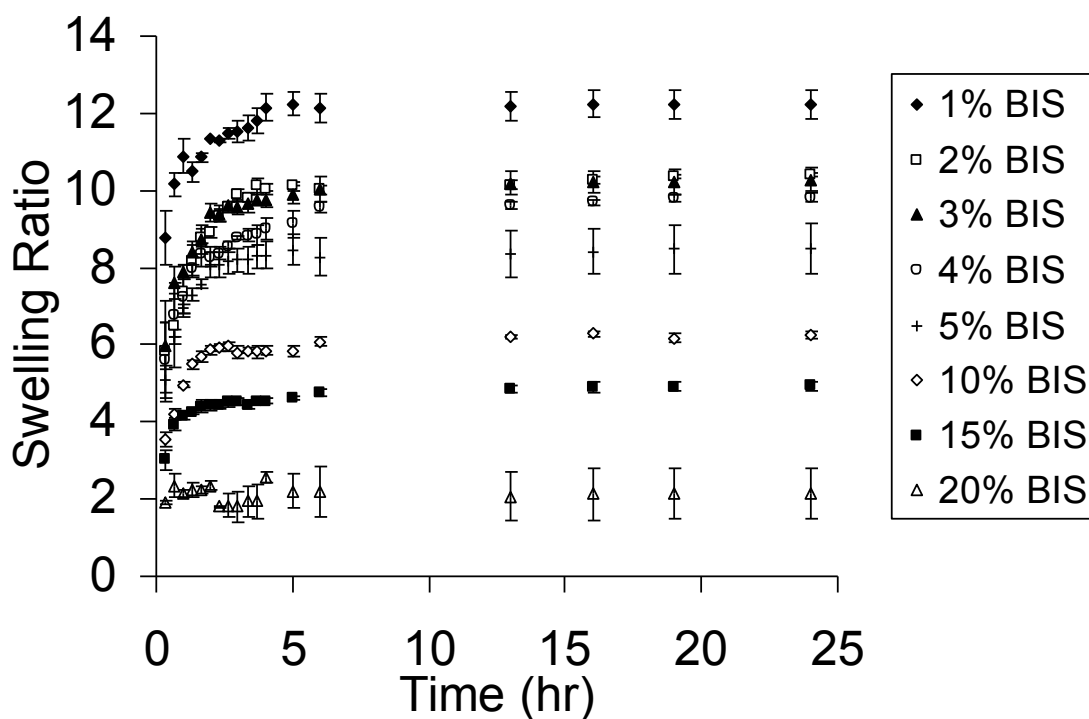
$$SP = 100 \times \frac{(M_t - M_0)}{M_0} = K_s e^{0.5t} \quad (\text{Equation 2})$$

where, $(M_t - M_0)/M_0$ is the swelling ratio as previously described, and the constant K_s is the swelling rate of the polymer sample.

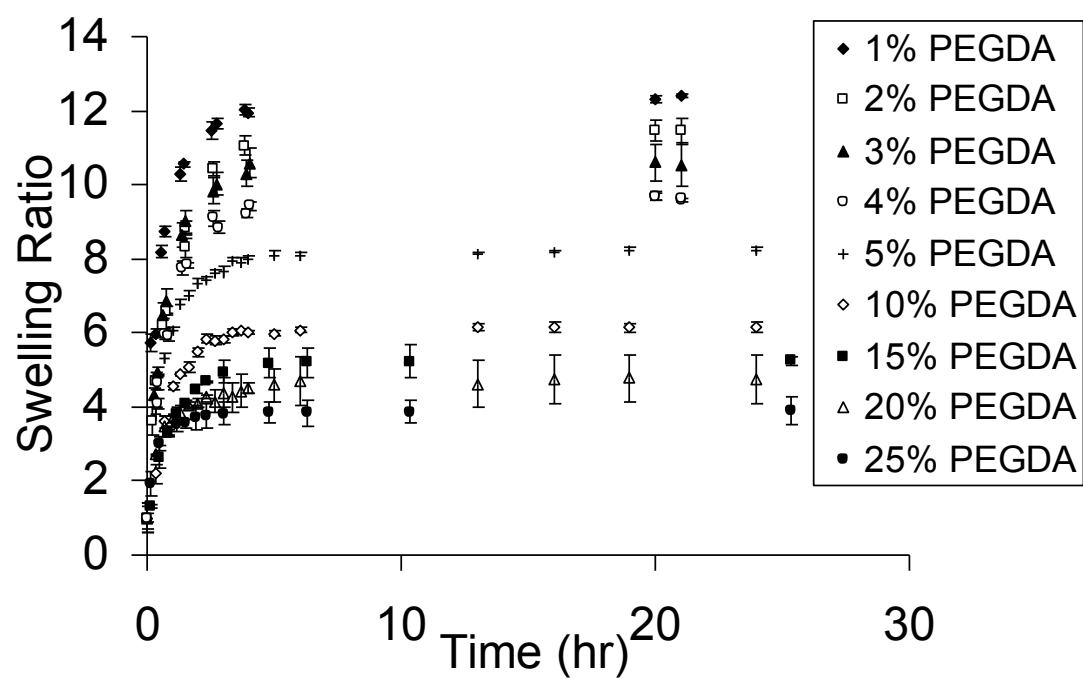
Swelling studies of 1-20 mole % BIS and 1-25 mole % PEGDA crosslinked gels in Figures 3a and 3b, respectively showed equilibrium swelling is obtained at 5

hours and is maintained without mass loss for the remainder of the 24 hours. Gel swelling is visually represented in Figure 3c. Increasing crosslink density reduced maximum swelling as shown in both Figures 3a and 3b. Swelling data was modeled by the Fickian swelling equation and the calculated values for K_s are shown in Table 2. K_s values are inversely related to crosslink density as expected for Fickian swelling.

A



B



C

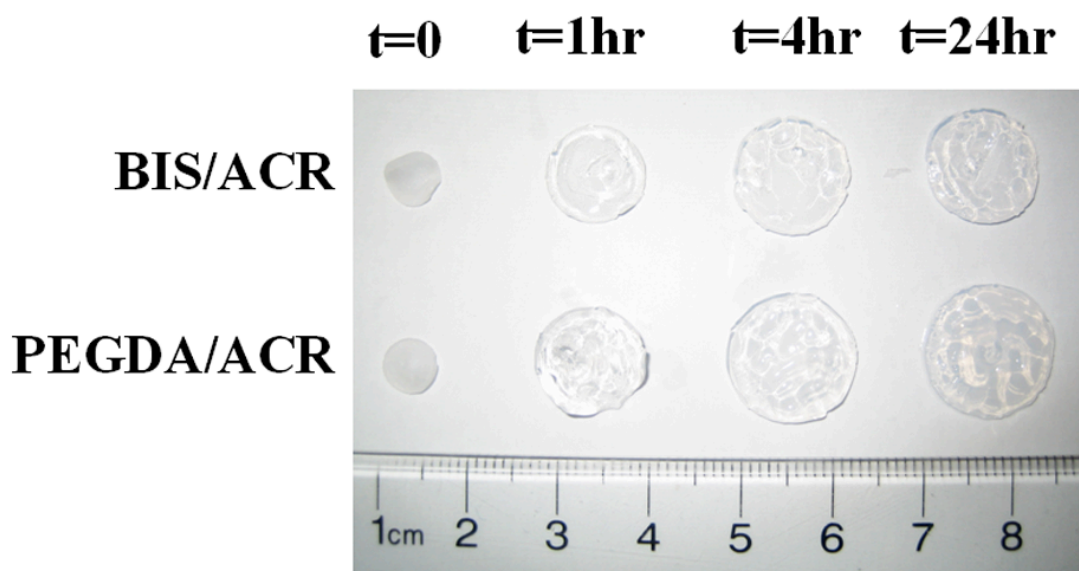


Figure 3. Swelling Behavior of BIS vs. PEGDA Crosslinked Hydrogels

A) Non-degradable gel: 1-20 mole % BIS crosslinked swelling factor over 24 hours. Crosslink density is inversely proportional to initial swelling rate and maximum swelling. Error reported as standard error of the mean.

B) Degradable gel: 1-25 mole % PEGDA crosslinked swelling factor over 24 hours. Crosslink density is inversely proportional to initial swelling rate and maximum swelling. Error reported as standard error of the mean.

C) Time lapse imaging show morphological changes of 10 mole % crosslinked PEGDA/ACR and BIS/ACR crosslinked gels as they swell in PBS over a 24 hour period.

Table 2: Calculated Fickian Swelling Constant, K_s

Increasing the crosslink density led to a decrease in K_s , as expected.

Cross-linker	Mole %	K_s (min ⁻¹)
BIS	1	30.87
	2	50.08
	3	44.56
	4	38.25
	5	40.62
	10	34.17
	15	17.45
	20	-
PEGDA	1	78.58
	2	68.83
	3	70.35
	4	62.73
	5	44.91
	10	38.96
	15	18.22
	20	14.70

Symbol (–) used when R^2 values are below 0.80.

Diffusion related issues of interest to this work are difficulties with substrate reaching the enzyme or product molecules diffusing out of the gel. Gels with higher swelling rates, notably at low crosslink densities, are not subject these diffusion related issues due to free movement of substrate and product molecules into and out

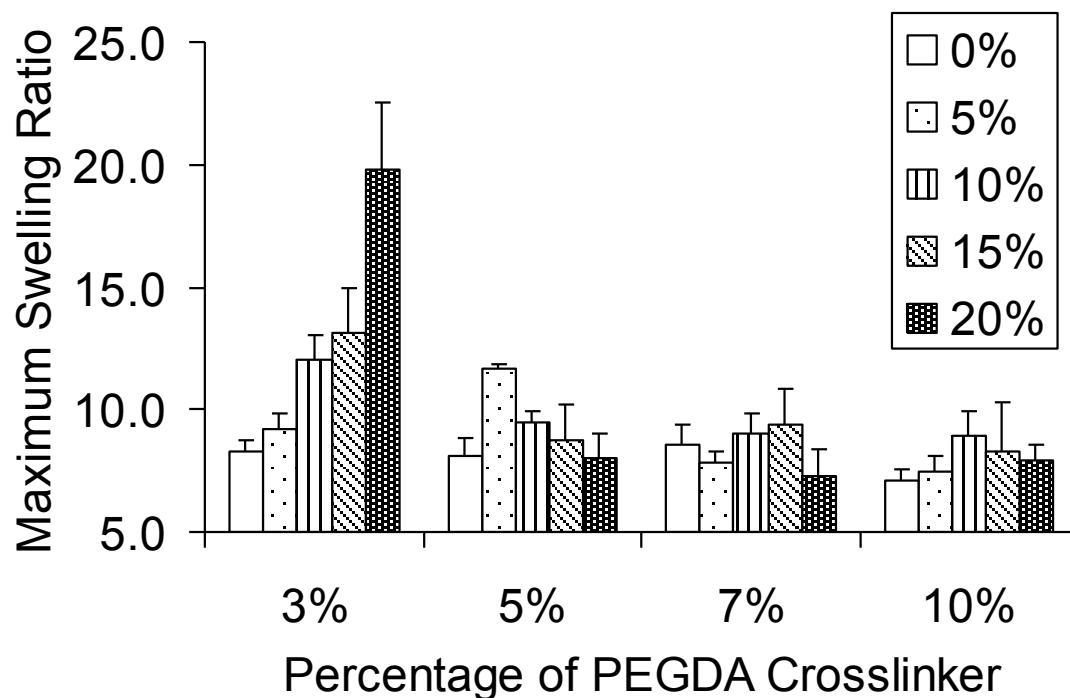
of the matrix. Biogels were fabricated through a drop cast method leading to films approximately 75 μm thick. At low crosslink densities, diffusion of dissolved substrate and product molecules was concluded not to be the rate-limiting factor of enzyme conversion. The rate-limiting step was determined to be enzyme conversion of substrate into product. Lumped into this factor is the binding of substrate, the conversion of substrate to product, and the enzyme release of the product molecule. At high crosslink densities diffusion may become a factor in the maximum velocity of enzymatic conversion of substrate into product.

2.4.1.2 Crosslink Density and Charged Monomer Studies

Swelling studies continued using MAPTAC (+) and AMPS (-) monomers to determine the relationship between these charged groups and maximum swelling. Swelling studies were performed for 1, 3, 7, and 10 mole % PEGDA crosslinked gels with 0, 5, 10, 15, and 20 mole % positive or negative monomer concentrations and are shown in Figures 4a and 4b respectively. Maximum swelling occurred after 5 hours of swelling in PBS media. Results shown are the swelling ratios determined at 24 hours. From these studies it can be seen that increasing crosslink density reduced maximum swelling as shown in both Figures 4a and 4b, regardless of the quantity of AMPS (-) or MAPAC (+) monomer additions. Adding AMPS (-) monomer to the hydrogel has a positive correlation to swelling ratio at low crosslink densities. As expected, the charged groups added to the low crosslink density gels allow for a large influx of PBS into the matrix. This is due to coulombic repulsion created by charge introduction into the matrix. Increasing the crosslink density decreases the maximum

swelling ratio regardless of the amount of negative monomer in the hydrogel. This is due to the higher density of crosslinks not allowing for the expansion of the matrix for PBS to enter. Small and large additions of MAPTAC (+) monomer to the hydrogel matrix, as seen in Figure 4b, have an equal positive effect on the matrix swelling ratio at low crosslink densities, again due to the coulombic repulsion of like charges. Increasing the crosslink density decreases the maximum swelling ratio regardless of the amount of positive monomer in the hydrogel.

A



B

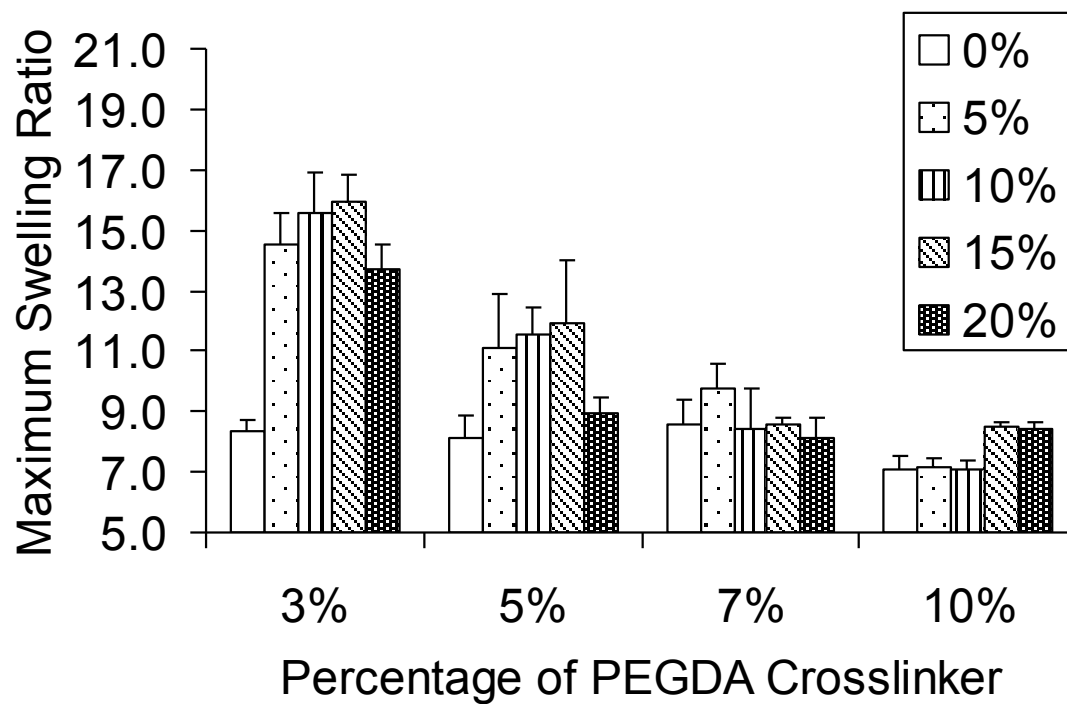


Figure 4. Swelling Behavior of Charged Hydrogels Crosslinked with PEGDA

A) Swelling ratio of 3, 5, 7, or 10 mole % PEGDA crosslinked hydrogels with 0, 5, 10, 15, or 20 mole % of negative monomer (AMPS). AMPS (-) monomer has a positive correlation to increased swelling ratio at low crosslink densities. Increasing the crosslink density decreases the maximum swelling ratio regardless of the amount of AMPS (-) monomer in the hydrogel. Error reported as the standard error of the mean.

B) Swelling ratio of 3, 5, 7, or 10 mole % PEGDA crosslinked hydrogels with 0, 5, 10, 15, or 20 mole % of positive monomer (MAPTAC). Small additions of MAPTAC (+) monomer to the hydrogel matrix have an equal positive correlation to increased swelling ratio at low crosslink densities to large MAPTAC (+) monomer additions. Increasing the crosslink density decreases the maximum swelling ratio regardless of the amount of MAPTAC (+) monomer in the hydrogel. Error reported as the standard error of the mean.

2.4.2 Degradation

2.4.2.1 Crosslinker type and Crosslink Density Studies

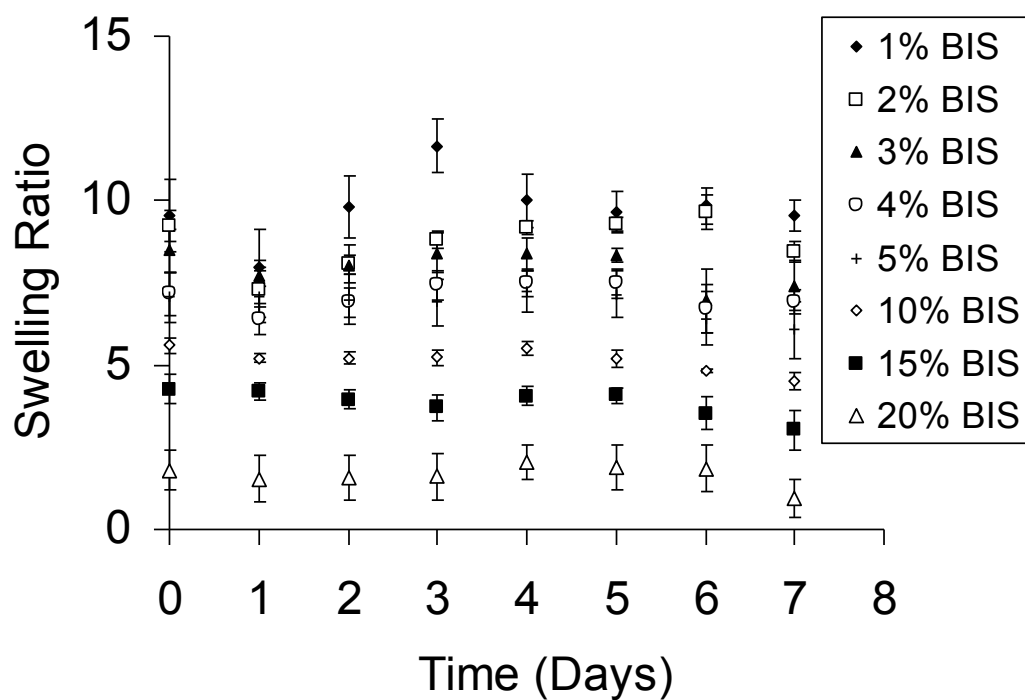
Hydrogel degradation was monitored through mass increase. As the PEGDA crosslinker hydrolyzed, the mesh size of the polymer matrix increased, allowing for an influx of water without shape deformation or measurable surface erosion as seen in Figure 5c. The swelling ratio was determined experimentally as described in Equation 1. BIS crosslinked matrixes did not degrade with the addition of NaOH as there are no hydrolyzable bonds. BIS crosslinker control studies were performed at 1, 2, 3, 5, 10, and 15 mole % for 7 days. PEGDA crosslinker degradation studies were performed at 1, 2, 3, 4, 5, 6, 7, 8, and 10 mole % for up to 12 days or for as long as the samples maintained mechanical stability and were able to be handled. Results of these studies are shown in Figures 5a and 5b, respectively.

Swelling and degradation results of the non-degradable control, BIS crosslinked gels, proved that size and structure was maintained throughout the experiment as seen in Figures 5a and 5c. As expected, no measurable mass gain or loss was recorded, demonstrating that crosslinks were not degraded. Figure 5c visually shows there was no degradation or erosion of the specimen when left in the 500 μ M NaOH degradation media for one week, and allows for comparison with similar crosslink density PEGDA gels. Similarly, to determine no mass loss of the specimen, each was dried after the experimented and determined to have no significant mass lost.

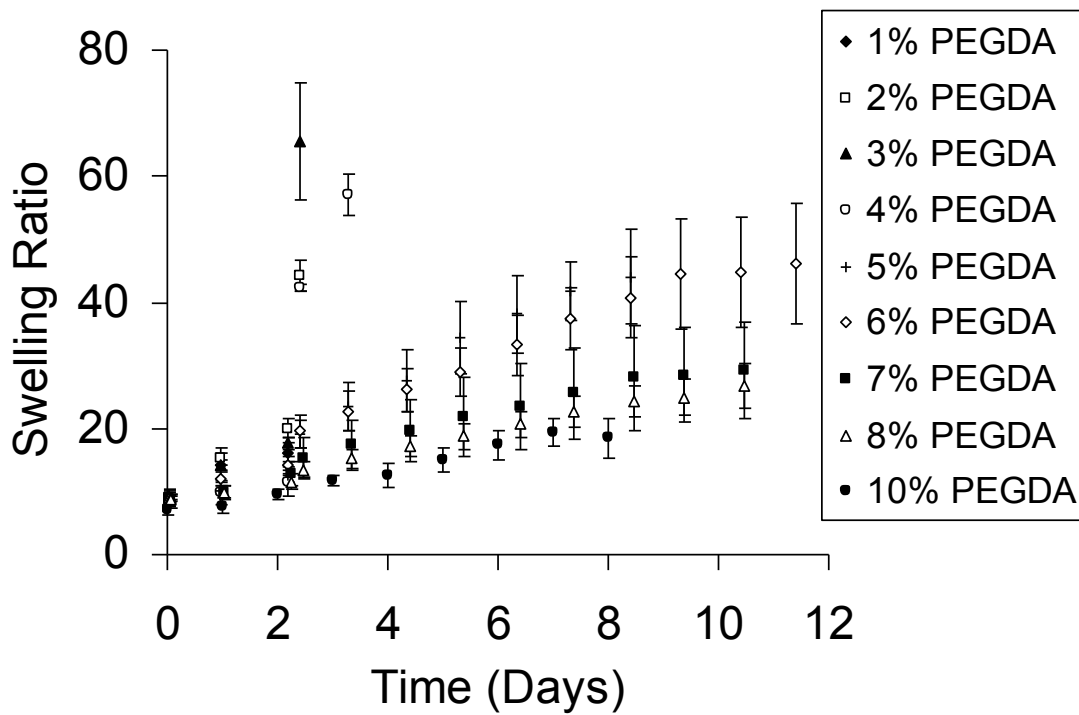
In contrast to the BIS crosslinked control gels, PEGDA crosslinked gels were degraded when the crosslinker was hydrolyzed by the 500 μ M NaOH media as seen

in Figures 5b and 5c. The gels maintained overall aspect ratios and shape despite becoming highly swollen as the crosslinks degraded (Figure 5c). When the PEGDA molecules were degraded, cavities within the matrix became larger, allowing for water molecules to diffuse more easily into the gel. As expected, increasing the matrix crosslink density decreased the degradation rate of the hydrogel matrix. Extensive hydrolysis was necessary to create the cavities for water diffusion. Degradation of all of the crosslinks led to complete dissolution of the gel into the media. The early stages of complete degradation can be seen in the 2, 3, and 4 mole % crosslinked hydrogels in Figure 5b. Large quantities of water invade the gel, swelling it to the point where the gel is drastically degraded in a short amount of time. Similar results were observed when the strength of the degradation media was increased tenfold to a 5 mM NaOH solution. In this instance, 1-10 mole % PEGDA gels were tested and swelled to a ratio of 40 and 50 times their original size, respectively, and degraded into the solution within a single day making results difficult to quantify.

A



B



C

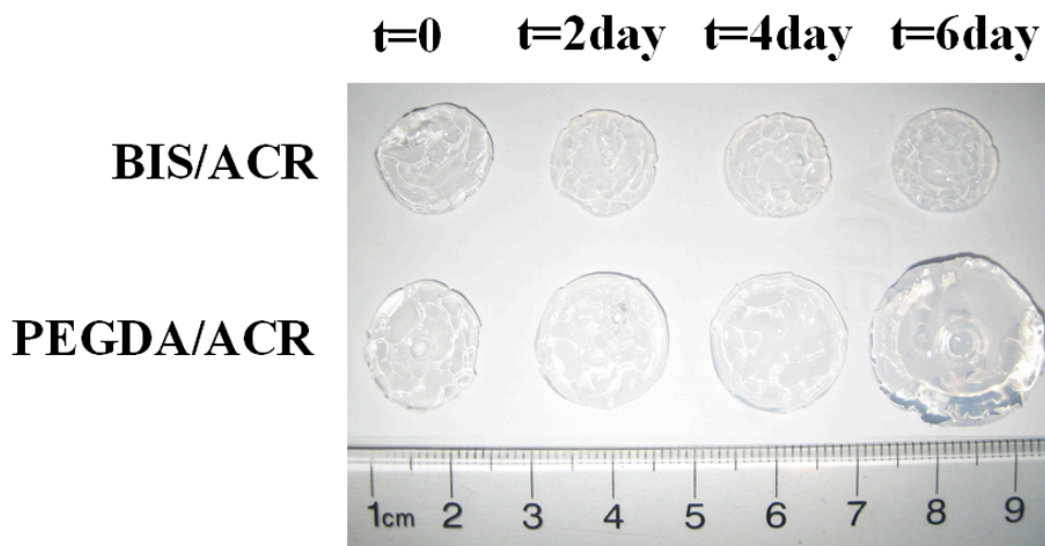


Figure 5. Degradation Behavior of BIS vs. PEGDA Crosslinked Hydrogels

A) 1-20 mole % crosslinked BIS/ACR gels degradation studies in 500 μM NaOH hydrolysis media. Crosslinks did not degrade, thus gels maintain original 24 hour PBS swollen state. $N = 3$ for all samples and all time points.

B) 1-10 mole % PEGDA crosslinked ACR gel degradation studies in 500 μM NaOH hydrolysis media. $N = 3$ for each sample at each time point.

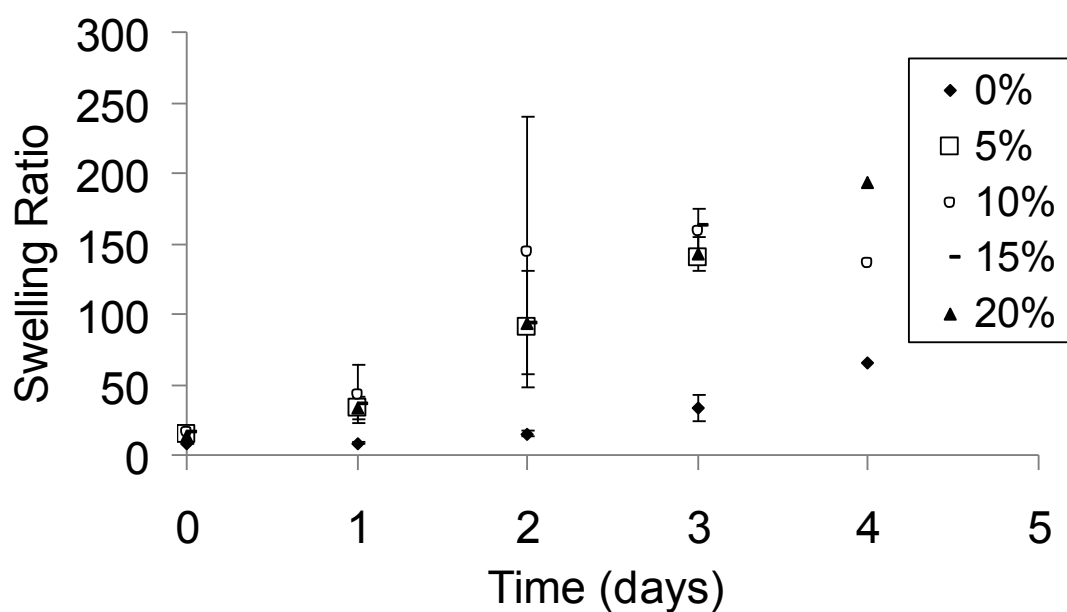
C) Time lapse imaging of morphological changes of 10 mole % crosslinked PEGDA/ACR and BIS/ACR crosslinked gels degrading in 500 μM NaOH over a 6 day time period.

2.4.1.2 Crosslink Density and Charged Monomer Studies

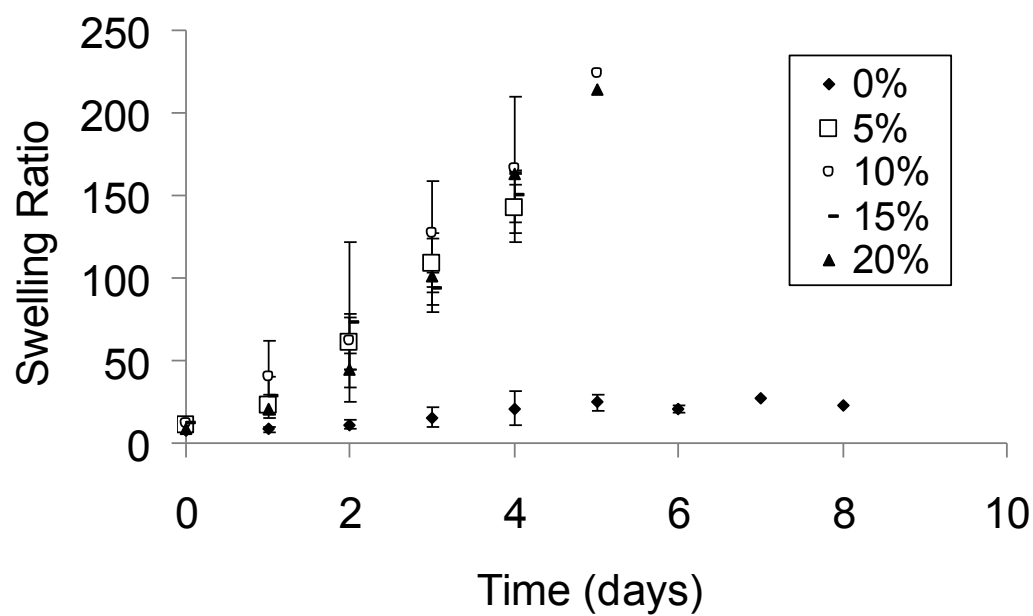
Similar to the previous section of crosslinker type and crosslink density studies, the following degradation data of hydrogel samples was monitored through mass increase. Again, as the PEGDA crosslinker hydrolyzes, the crosslink density decreases, allowing for an influx of water without shape deformation or measurable surface erosion. Swelling ratios were determined by Equation 1. Results from the PEGDA crosslink density studies in the previous section were used as controls to

compare degradation rates in hydrogels with charged monomer moieties. Degradation studies were performed with PEGDA crosslinked gels to contain 3, 5, 7 and 10 mole % crosslinking and 5, 10, 15 or 20 mole % MAPTAC (+) (Figure 6a-6d) or AMPS (-) (Figure 7a-7d) monomer moieties. These degradation results are reported in Figures 6 and 7, respectively.

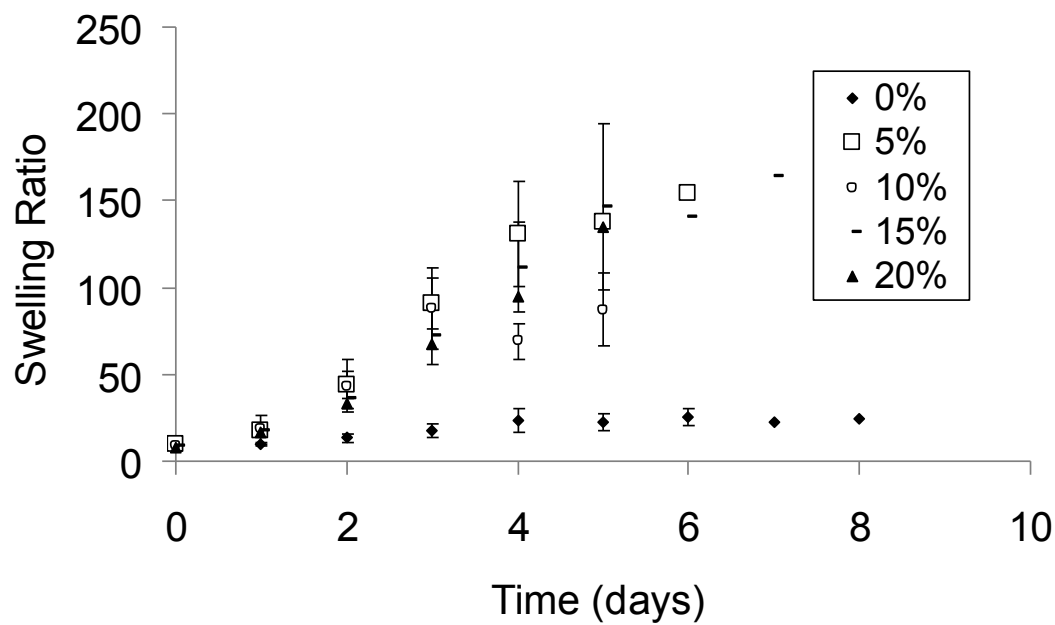
A



B



C



D

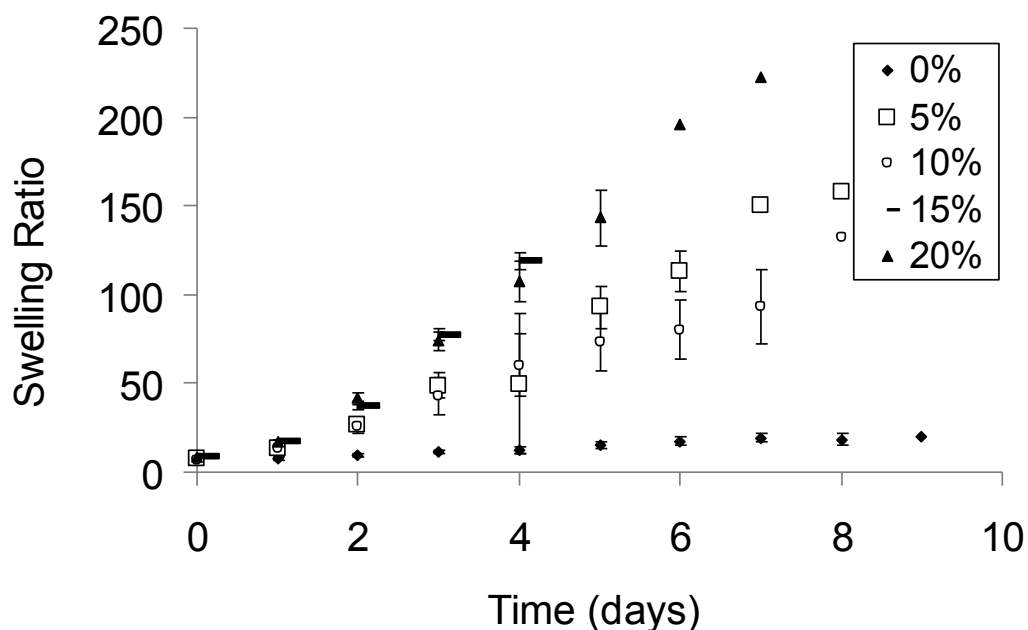


Figure 6. Degradation Behavior of Positively Charged Hydrogels

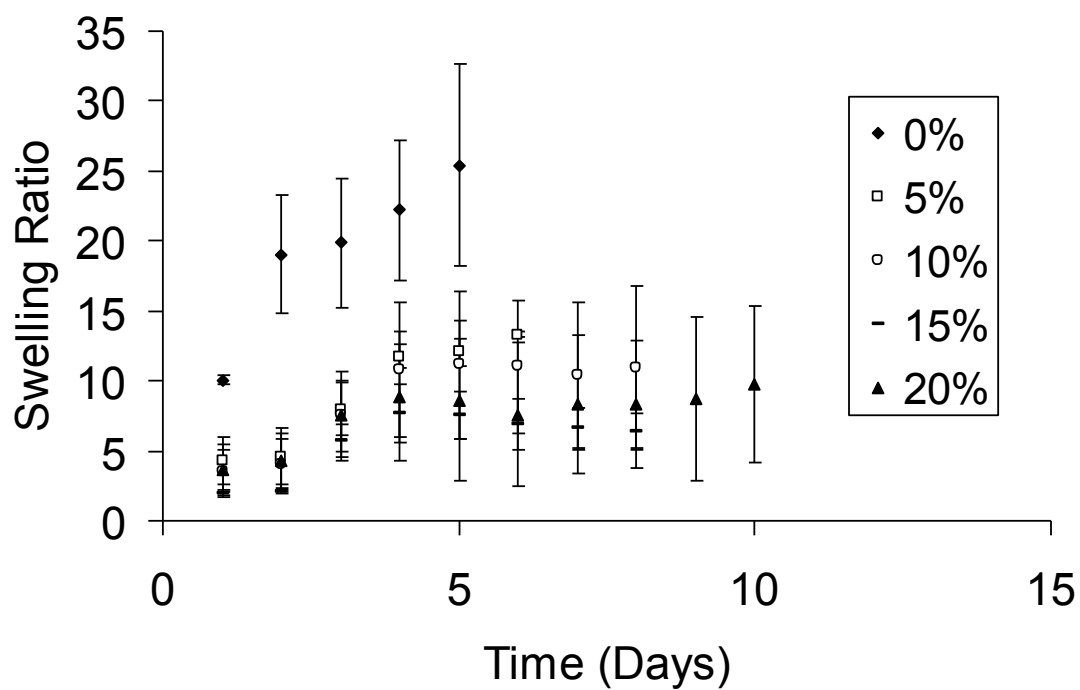
Degradation curves containing ACR and 0-20 mole % MAPTAC (+) monomer amounts. Error bars for N = 3 no error bars equates to N = 2.

- A) 3 mole % Crosslinked
- B) 5 mole % Crosslinked
- C) 7 mole % Crosslinked
- D) 10 mole % Crosslinked

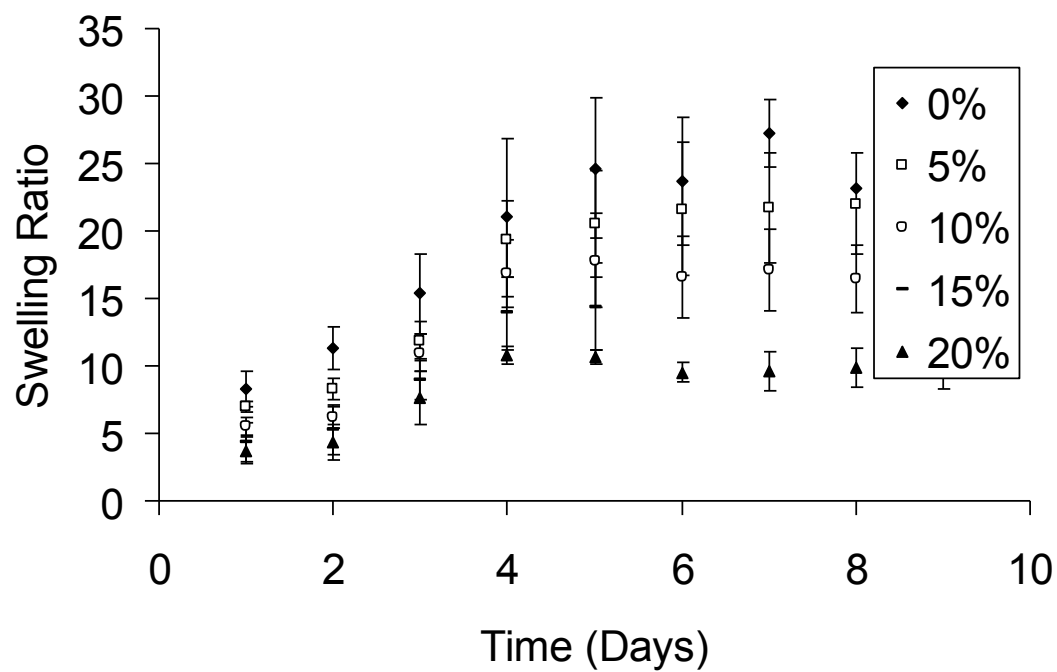
The addition of MAPTAC (+) monomer increased the degradation rate of the hydrogel. This is shown by the increase in the slope of swelling ratios verified in Figure 6a-6d. At low crosslink densities (Figures 6a-6c), the amount of MAPTAC (+) monomer to ACR had no quantifiable relationship to the increased degradation rate. At 10 mole % crosslink densities there was a positive correlation between monomer moiety and increased degradation rate as seen by the increased slopes of degradation in Figure 6d. This degradation behavior is due to the MAPTAC (+) monomers coulombic repulsion from each other, allowing more NaOH to invade the matrix and

hydrolyze the ether groups of the PEGDA crosslinker at a more rapid pace. The positively charged groups both aid in diffusion of solvent into the matrix while also improving gel mechanical stability, allowing for accurate measurements of swelling at swelling ratios on the order of 100.

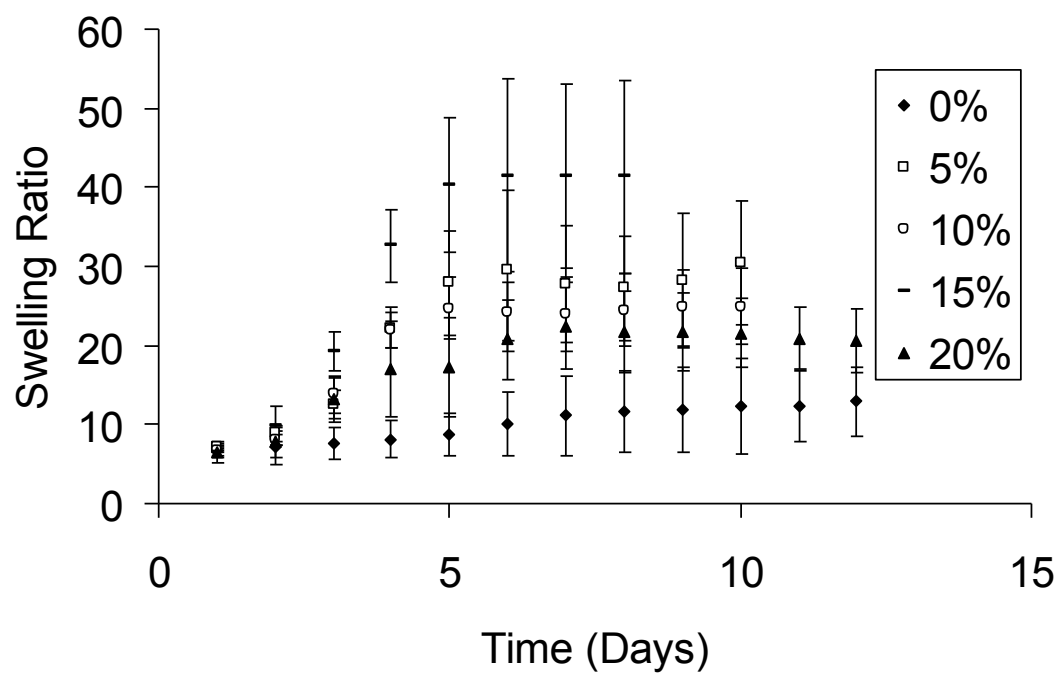
A



B



C



D

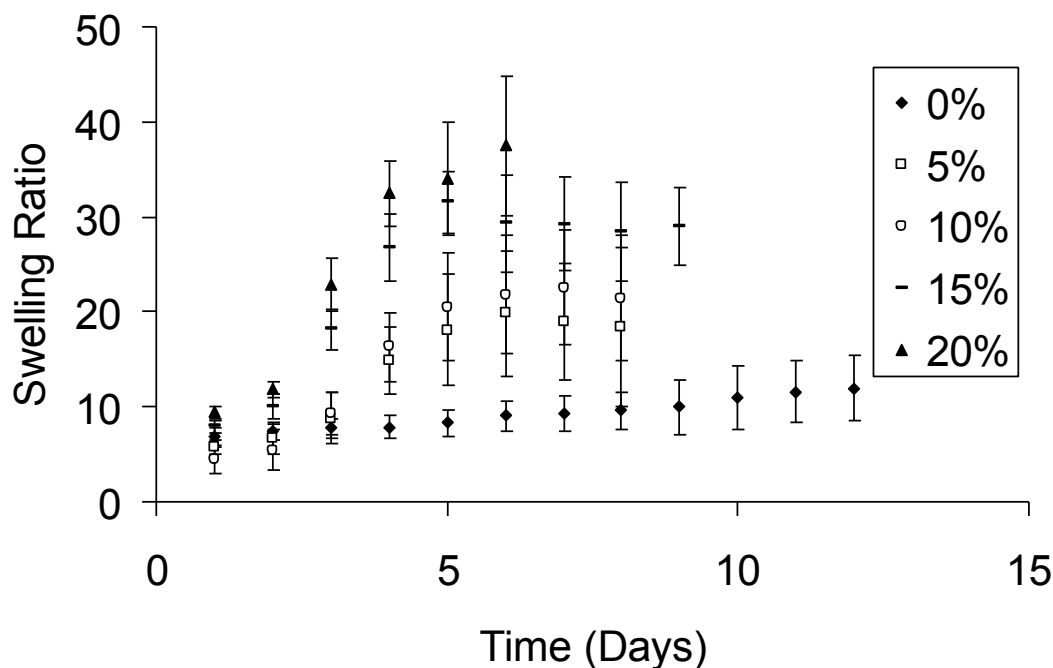


Figure 7. Degradation Behavior of Negatively Charged Hydrogels

Degradation curves containing ACR and 0-20 mole % AMPS (-) monomer amounts. Error bars for $n = 3$ no error bars equates to $n = 2$.

- A) 3 mole % Crosslinked
- B) 5 mole % Crosslinked
- C) 7 mole % Crosslinked
- D) 10 mole % Crosslinked

A variation of this swelling behavior was observed in the results of AMPS (-) monomer moiety addition to the matrix as seen when comparing Figures 7a-7d. At 3 and 5 mole % crosslink density (Figure 7a and 7b, respectively), the addition of AMPS (-) monomer decreased degradation rates. It is thought that this behavior is caused by strong chemical potential gradient shielding against the penetration of free negatively charged OH^- molecules to the PEGDA degradation sites. This effectively reduces the number of bonds that can be degraded within a set time frame and increases degradation time. Figures 7c and 7d of higher crosslink density hydrogels, 7

and 10 mole % PEGDA, respectively, showed a similar trend as seen in the addition of positively charged monomers, where the charge groups once again exhibit coulombic repulsion and decrease diffusive barriers, leading to increased swelling and degradation. Only noticeable in Figure 7d is the positive correlation between increases in AMPS (-) monomer content and degradation rate. Large errors can be found on all low (less than 3 mole %) crosslink density gels as the mechanical stability of these gels and morphological alterations due to the drying step alter diffusion distances. For higher crosslinked gels (i.e. 5, 7 and 10 mole %) the same drying effect was not observed and the hydrogels were not prone to morphological defect.

Degradation study results of 3, 5, 7 and 10 mole % PEGDA crosslinked gels with 5, 10, 15 or 20 mole % MAPTAC (+) monomer indicate decreased time to total gel degradation with increased positive monomer moieties. Degradation study results of 3, 5, 7 and 10 mole % PEGDA crosslinked gels with 5, 10, 15 or 20 mole % AMPS (-) monomer indicated two different degradation phenomena: 1) at low crosslink density, the addition of negative monomer decreased degradation rates, and 2) at higher crosslink densities, the coulombic repulsion of charge groups decreased lead to increases in swelling and degradation. It is also noted that there is a positive correlation between increased negative monomer content and degradation rate at high crosslink densities. Both positively and negatively charged groups seemed to aid in gel mechanical stability, allowing for accurate measurements of the swelling ratio on the order of 100.

2.4.3 Dynamic Mechanical Analysis

DMA and swelling data described in Table 3 were collected from 2.5 to 15 mole % BIS crosslinked gels to determine the linear elastic and the strain hardening moduli of the gels. Gel mechanical properties are useful to compare single component gel toughness and performance to gels containing positive or negative monomer moieties randomly copolymerized with ACR monomers. DMA was performed in compression and submersion mode using a multi-strain sweep of 0-5% sample height deformations at 1 Hz. Sample height was determined, separately, for each gel, at each state of swelling, and 5% of the height was determined as the maximum sample deformation. Data was obtained for gels “as synthesized” and were then tested at various states of swelling, including fully swollen in PBS for 4 hours. At least 3 gels of each monomer and crosslinker type were fabricated and tested to obtain the linear elastic and strain hardening moduli. Enzymatic ONPG conversion studies were performed while the gels are swollen. Therefore, gel properties relative to the swollen state were most informative in determining the relationship between gel mechanical properties and enzyme stability. The linear elastic modulus is determined using the 0-1% strain range and is the slope of the DMA stress-strain graph in this range. The strain hardening modulus is found in the 4-5% strain range, where the stress-strain behavior begins to become exponential and gives important insight into the gel behavior prior to failure. Error is reported in standard error of the mean (SEM). It should be noted here that there was no measurable loss of buffer in the various states of swelling due to the deformation through compression of the hydrogel matrix.

Table 3: Mechanical Properties as Determined through DMA

BIS Crosslink Density	As Synthesized		Swelling Ratio Fully Swollen ÷ As Synthesized	Fully Swollen	
	Linear Elastic Modulus (Pa)	Strain Hardening Modulus (Pa)		Linear Elastic Modulus (Pa)	Strain Hardening Modulus (Pa)
2.5 %	40 +/- 5	178 +/- 73	1.491 +/- 0.027	14 +/- 2	32 +/- 6
5 %	45 +/- 10	230 +/- 120	1.287 +/- 0.004	22 +/- 3	72 +/- 8
10 %	54 +/- 5	320 +/- 74	1.281 +/- 0.021	28 +/- 6	86 +/- 6
15 %	65 +/- 7	307 +/- 22	1.183 +/- 0.026	20 +/- 7	75 +/- 12

Swelling the hydrogels effectively lowered both the linear elastic modulus and the strain hardening modulus in all fabricated gels as seen in Table 3. Increased swelling is seen at low crosslink density as described in the previous swelling section of this thesis is also seen here in the swelling ratio term of Table 3. The dynamic mechanical analysis of the hydrogels showed increased linear elastic and strain hardening moduli at higher crosslink densities, as expected.

Results of PEGDA crosslinked gels with 0-30 mole % AMPS (-) or MAPTAC (+) monomer are seen in Tables 4-7. The linear elastic and strain hardening moduli for each gel was determined in hydrogel samples of 10, 50 and 100% of the max swelling from a dried state as shown in Figure 8. Linear elastic moduli were calculated using slope data acquired relating to the 0-1% sample strain. As expected, increased swelling showed decreased overall linear elastic moduli. Strain hardening moduli were calculated in samples that showed change in slope in the 4-5% strain zone. In Figure 8 for example, strain hardening moduli were calculated for 10 and

50% of max swelling but the max swelling sample exhibited no quantifiably relevant slope change, thus had no discernable strain hardening in the 4-5% strain area.

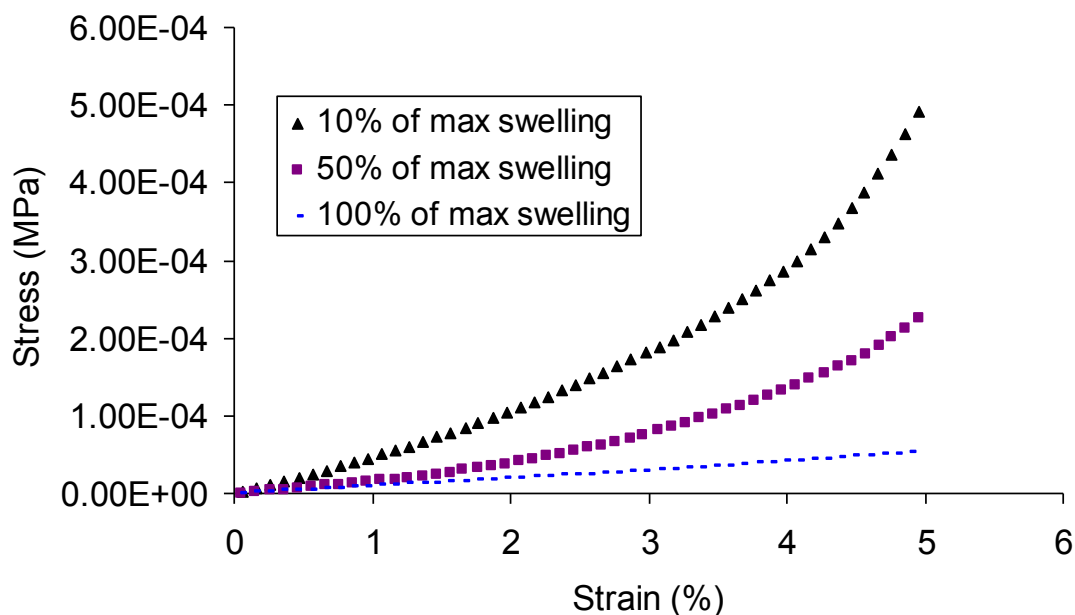


Figure 8. Stress vs. Strain DMA Results in Various States of Swelling.

Stress vs. strain of 15 mole % PEGDA crosslinked hydrogels at 10, 50 and 100 % of max swelling.

As expected, increased crosslink density increased both the linear elastic and the strain hardening moduli, therefore continued investigations focused on the AMPS (-) and MAPTAC (+) monomer content effects on bulk mechanical properties. The linear elastic and strain hardening moduli (LEM and SHM), Tables 4 and 5 respectively, for gels containing 0-30 mole % AMPS were determined in “as synthesized” state and after 5 hrs of swelling in PBS until maximum swelling had been reached, denoted by “fully swollen.” Error in the tables is reported as standard error of the mean (SEM).

Table 4: LEM of 10% Crosslinked 0-30 % AMPS (-) Monomer

% (-) monomer	As Synthesized		Fully Swollen	
	LEM (Pa)	SEM	LEM (Pa)	SEM
0%	64.63	4.50	28.28	5.74
2.5%	65.35	19.26	22.07	2.03
5.0%	54.40	18.23	8.76	2.23
10.0%	42.70	25.04	4.84	1.70
15.0%	33.14	0.52	14.16	1.01
20.0%	22.51	1.87	18.77	0.03
25.0%	40.23	17.07	33.40	2.83
30.0%	12.45	3.16	20.70	6.29

Table 5: SHM of 10% Crosslinked 0-30 mole % AMPS (-) Monomer

% (-) monomer	As Synthesized		Fully Swollen	
	SHM (Pa)	SEM	SHM (Pa)	SEM
0%	226.11	10.59	86.48	6.32
2.5%	149.03	39.10	64.02	3.85
5%	114.00	12.48	41.40	20.23
10%	88.10	17.53	46.80	21.47
15%	172.09	46.79	48.25	18.09
20%	62.03	9.91	41.35	20.23
25%	173.69	79.34	98.67	52.78
30%	92.84	28.61	86.43	17.68

Gels in a fully swollen state showed reduced LEM and SHM as expected due to the increased PBS content. Interestingly, increasing the density of AMPS (-)

monomer decreased the measured LEM. This is presumed to be a factor of unavoidable swelling due to PBS content within the tested hydrogel construct. Submersion compression clamp DMA measurements are made with a small amount of PBS in the cup in order to deter gel adhesion, due to suction forces, to the apparatus. It should also be noted that increased MAPTAC (+) had a similar effect on the LEM (Tables 6 and 7). Strain hardening modulus, SHM, showed no distinct trend based on the MAPTAC (+) or AMPS (-) monomer additions and remained relatively constant in the “as synthesized” gels and lower but constant in the “fully swollen.” Error in the tables is reported as standard error of the mean (SEM).

Table 6: LEM of 5% Crosslinked 15-30 mole % MAPTAC (+) Monomer

% (+) monomer	As Synthesized		Fully Swollen	
	LEM (Pa)	SEM	LEM (Pa)	SEM
15%	58.28	19.58	5.75	2.56
20%	46.54	22.20	6.68	0.55
25%	43.42	20.53	4.38	2.53
30%	32.22	20.96	9.82	0.04

Table 7: SHM of 5% Crosslinked 15-30 mole % MAPTAC (+) Monomer

% (+) monomer	As Synthesized		Fully Swollen	
	SHM (Pa)	SEM	SHM (Pa)	SEM
15%	107.56	26.36	89.53	17.05
20%	169.66	27.30	110.90	66.45
25%	153.49	5.01	85.39	40.72
30%	88.70	47.29	34.42	28.10

2.5 Conclusions

The fabricated ACR gels crosslinked with BIS and PEGDA showed Fickian swelling in PBS media. PEGDA crosslinked gels swelled more than BIS crosslinked gels, especially at high crosslink densities. Increased crosslink density decreased the maximum swelling and decreased the swelling rate, K_s , due to a tighter hydrogel mesh. These results led to the conclusion that slower diffusion may affect the enzyme's ability to convert substrate into product at high crosslink densities. At low crosslink densities the rate-limiting factor is the process of enzyme conversion into substrate. AMPS (-) monomer has a positive correlation to increased swelling ratio at low crosslink densities. Increasing the crosslink density decreases the maximum swelling ratio regardless of the amount of AMPS (-) monomer in the hydrogel. Small additions of MAPTAC (+) monomer to the hydrogel matrix have an equal positive correlation to increased swelling ratio at low crosslink densities to large MAPTAC (+) monomer additions. Increasing the crosslink density decreases the maximum swelling ratio regardless of the amount of MAPTAC (+) monomer in the hydrogel.

The fabricated ACR gels crosslinked with BIS and PEGDA compared to the degradation of PEGDA gels with BIS gels. At high crosslink densities PEGDA gels show lower swelling over time. The increased PEGDA density as described in the swelling section of this work caused a decrease in the swelling rate making it more difficult for solution to diffuse into the gel. A large number of these crosslinks must be degraded to increase the diffusion of degradation media into the gel. With fewer hydroxyl molecules reaching the hydrolyzable bonds within the PEGDA crosslinker, the degradation was slowed. Results of 3, 5, 7 and 10 mole % PEGDA crosslinked gels with 5, 10, 15 or 20 mole % MAPTAC (+) monomer indicated increased gel degradation rates with increased MAPTAC (+) monomer moieties. Degradation study results of 3, 5, 7 and 10 mole % PEGDA crosslinked gels with 5, 10, 15 or 20 mole % AMPS (-) monomer indicated two different degradation mechanisms; 1) at low crosslink density the addition of AMPS (-) monomer decreased degradation rates, 2) at higher crosslink densities the coulombic repulsion lead to increased swelling and degradation. Both positively and negatively charged groups seemed to aid in gel mechanical stability, allowing for accurate measurements of the swelling ratio on the order of 100.

Swelling the hydrogels lowered both the LEM and the SHM in all fabricated gels as expected due to the increased PBS content. Similarly, increasing the density of MAPTAC (+) or AMPS (-) monomer decreased the measured LEM. This is again presumed to be a factor of the absorbed PBS.

Chapter 3: Biogel Characterization at Different Crosslink

Densities

3.1 Objectives

To develop and optimize the fabricated biogels, it was necessary to determine entrapment effects on enzyme kinetics. The four main objectives for characterization of entrapped enzyme kinetics at different crosslink densities were: 1) determine the relationship between crosslinker type (BIS, non-degradable and PEGDA, degradable) and lactase activity post-entrapment: 2) establish the influence of crosslinker density on entrapped enzymes, and 3) determine the repeatability of producing small molecules over a two day study, and 4) characterize the matrix ability to protect the enzyme when the environment is perturbed to a pH of 8. To achieve these objectives, β -galactosidase (lactase) enzyme was entrapped within hydrogel matrices of ACR crosslinked with BIS (non-degradable) or PEGDA (degradable) to create biogels. These biogels were compared to each other to determine an optimal environment for enzyme entrapment and activity retention in the 7-8 pH range.

Confocal imaging was used to determine the distribution of enzyme within the gel in order to compare clustering behavior with crosslink density of PEGDA crosslinked biogels. Enzymatic tests performed at 2, 24, and 48 hours aim to prove repeatable synthesis and enzyme stability over the two day study. Protection studies use a pH challenge of 8 to prove the efficiency of highly crosslinked networks over solution based enzyme activity retention. At a pH of 8 some positive control, free

enzyme in solution, should remain active for comparison with the fabricated biogels. This pH is also applicable for use in the charged monomer studies, allowing the AMPS (-) to remain highly deprotonated and the MAPTAC (+) to remain highly protonated.

3.2 Introduction

The goal of this work is to extend beyond the current enzymatic stabilization methods including additive stabilization, chemical or physical modification of the enzyme and current entrapment and immobilization techniques (8-11, 13, 28) to create a biogel complex that can be easily tailored to a desired enzyme based on its size and isoelectric point (pI). These methods have the potential to be generic, bioinspired, efficient, repeatable and allow for the synthesis of high-purity biomolecules with long-term stability. Biogel optimization was carried out by varying crosslink density of the entrapping matrix; thereby eliminating the need for genetic or covalent enzyme modification. The formed biogel complexes have the enzymatic ability to produce desired biological small molecules. A library of hydrogel matrices was prepared and compared to create favorable environmental conditions for any enzyme. This catalog includes various crosslink density matrices with degrading and non-degrading crosslinkers. Information gathered from the library can be used to create optimal constructs for immobilization and stabilization of the enzymes contained within the biogels.

This concept was demonstrated using hydrogel matrices of ACR crosslinked with BIS (non-degradable) or PEGDA (degradable). The test enzyme, β -galactosidase (lactase), a digestive enzyme which degrades lactose substrate into glucose and

galactosidase, was entrapped within the matrix to create the biogel. Ortho-nitrophenyl- β -D-galactopyranoside (ONPG) is a compatible substrate to lactase which, when catalyzed by lactase, yields one galactosidase molecule and one ortho-nitrophenol (ONP) molecule. ONP readily absorbs light at $\lambda = 420$ nm, making it a simple model enzyme system to utilize during crosslinker type and density optimization studies to report lactase activity. Optimization studies focused on two main objectives: maintaining enzyme activity through the gel entrapment procedure while also protecting the enzyme in non-ideal environments. Positive controls in this work aim to show that no enzyme is lost through the wash cycles and that the ACR/PEGDA biogels show promise in being an abiotic, generic, and efficient entrapment matrix when compared to alginate gels.

3.3 Methods

3.3.1 Materials

Acrylamide (ACR), *N,N'*-methylenebisacrylamide (BIS), poly(ethylene glycol)diacrylate (Mn=700 PEGDA), ammonium persulfate (APS), *N,N,N',N'*-tetramethylethylenediamine (TEMED), ortho-nitrophenyl- β -D-galactopyranoside (ONPG), phosphate buffered saline (PBS) and β -galactosidase (lactase, 476kDa) from *kluyveromyces lactis* were purchased from Sigma Aldrich and were used as received except for PEGDA which was first filtered through an inhibitor removal column prior to application. NHS-Rhodamine, borate buffer, and buffer exchange spin columns were purchased from Pierce[®] and used as described in the Pierce[®] NHS-Rhodamine Antibody Labeling Kit for confocal microscope imaging of biogels. A

Nipkow (spinning) disk-equipped Olympus IX81 fluorescent confocal microscope with a 10X objective at ex/em 552nm/575nm was used to determine protein location within gels. A plate reader (SpectraMax(R) M5, from Molecular Devices) measured absorbance at $\lambda = 420$ nm every 20 seconds for 10 minutes. The bound enzyme degraded ONPG substrate into product ONP. ONP absorbs light at $\lambda = 420$ nm. This allowed for the determination of ONP concentrations over time and was used to prove the enzymatic entrapping as a viable concept. This was also used to optimize enzymatic protection through entrapment using highly crosslinked networks.

3.3.2 Confocal Microscopy

β -galactosidase was diluted to 2 mg/mL using a NanoDrop ND-1000 Spectrophotometer. The PBS buffer was replaced with borate buffer, pH 8.5, using buffer exchange spin columns. To a vial of NHS-Rhodamine dye reagent, 500 μ L of the 2 mg/mL lactase in borate buffer was added and incubated for one hour to allow for protein labeling to occur. N-hydroxysuccinimide (NHS) binds to free amine groups on the lactase allowing the rhodamine dye to be chemically linked to the enzyme. The labeled enzyme was purified by running the samples through spin columns at 1000 rpm. The collected samples were stored at 4 °C until used for confocal imaging. The labeled enzyme was entrapped within 30 μ L of drop cast biogel in dilutions described for enzymatic activity studies in section 3.3.4. There were a total of 3 slides per crosslink density (5, 20, and 40 mole %) being studied. The roughly 75 μ m thick films were washed for two hours in PBS and then excited at 552 nm and imaged at the emission wavelength of 575 nm with a fluorescent confocal

microscope using the 10X objective. Three 10 μm depth images were taken of each slide and analyzed in ImageJ for bright spots and intensity measurements.

3.3.3 Positive Control Studies

3.3.3.1 Solution and Chemical Fixation

Positive controls provided proof of efficacy of the entrapment and protection procedures. Solution based and chemical fixation methods were used to determine maximum enzyme kinetics. Solution based kinetics without gels were determined by diluting lactase with PBS to match quantities utilized in biogel studies. Approximately 50 active enzyme units, determined through manufacturer's quantification, were entrapped within each biogel. As the stock enzyme aged, the volume was not altered though the active enzyme units decreased. Positive controls were run with each set of biogels, each with comparably aged enzyme for comparison. The diluted samples were refrigerated at 4 °C in PBS for 2, 24, and 48 hours as well as 8 and 15 days to determine the solution based activity retention over extended periods of time. These studies were performed with and without the addition of activated cover slides. Activated cover slides were utilized as all biogels were fabricated on top of glutaraldehyde activated cover slides to prevent thin film lift off from the base cover slide. Dissimilar from gel entrapment studies, no wash steps were used as the enzyme in solution would have been removed during the removal of the wash buffer.

Chemical fixation enzyme kinetics were determined by dropping 30 μL of diluted enzyme solution onto glutaraldehyde activated cover slips. The solution was evenly distributed with the addition of a top glass cover slide. After 20 minutes the

top slide was removed and the bottom slide was washed in PBS for 2 hours before measuring the kinetic parameters. The calculated conversion rates, specifically measuring the Michaelis–Menton constants, related only to enzyme adsorbed and chemically fixed to the glass slide.

Kinetic parameters were determined in solution based and chemically fixed positive controls by placing the samples in 6 well plates and measuring enzymatic catalytic conversion of substrate into product. Specifically, ONPG substrate conversion was measured through ONP production ($\lambda = 420$ nm). This was repeated for 0.1, 0.2, 0.4, 1, and 10 mg ONPG/mL PBS substrate concentrations. Lineweaver-Burk plots were created to determine the Michaelis-Menten constant, K_m , and the maximum reaction velocity, V_{max} .

3.3.3.2 Enzyme Diffusion out of Biogel

Prior to determining biogel enzymatic kinetic parameters, free enzyme and unreacted reagents were washed from the matrix. Enzyme diffusion out of the biogels was determined through subsequent washes. Crosslink densities of 15, 20 and 25% gels were synthesized, washed, and tested for initial enzymatic kinetic parameters, K_m and V_{max} . Diffusion studies included: consecutive PBS washes every 15 minutes for 45 minutes, a timed diffusion wash for 3 hours, and a timed diffusion wash for 24 hours. Wash buffer (containing PBS, free enzyme and unreacted chemicals) was removed from the gel samples, placed in 6-well plates, and tested for conversion by introducing 0.5, 0.1, 0.2, 0.5, and 5 mg/mL ONPG in PBS and recording the absorbance at $\lambda = 420$ nm over 10 minutes. Lineweaver–Burk plots were constructed

to determine V_{\max} and K_m of various states of wash buffer so that active enzyme diffusion out of the biogel could be detected.

3.3.3.3 Enzyme Entrapped in Alginate Hydrogels

Alginate gels were fabricated to prove the superior efficacy of the biogels in relationship to a current entrapment method. Alginate gels are fabricated from biological monomers which form ionic crosslink with the introduction of divalent calcium ions. They typically have poor cavity control and, because of the ionic crosslinking, degrade in buffers containing monovalent cations (35-37).

Alginate gels for these studies were produced by dissolving sodium alginate in deionized water to 1, 2, and 3 % weight/volume. Blank control gels, containing no enzyme, were fabricated from this stock. Biogels contained 12.5 μL of active enzyme stock, as purchased, per mL of alginate solution. Alginate gels were formed by drop pipetting 30 μL of the prepared alginate solutions from a height of 6 to 12 inches into a solution of 50 mM calcium and allowed to incubate in solution for 5-10 minutes. Single spherical gels of 30 μL were formed upon contact of the alginate with the calcium ions in the calcium chloride solution.

PBS will dissolve alginate gels as the calcium ions are replaced by monovalent potassium ions. Therefore multiple test solutions were utilized to determine alginate gel lactase kinetics. Alginate biogels were tested in the following substrate solutions: ONPG dissolved in PBS, ONPG dissolved in distilled water, and ONPG dissolved in 50 mM calcium chloride solution altered to a pH of 7.4 with the addition of HCl. Kinetic parameters were determined in these solution settings by the creation of Lineweaver-Burk plots of 0.1, 0.2, 0.4, 1, and 10 mg/mL ONPG in the

desired solvent. Positive controls of free enzyme conversion of ONPG in PBS, distilled water, and in calcium chloride were also determined to compare the various K_m and V_{max} 's acquired to the alginate entrapment studies.

3.3.4 Enzyme Activity

Hydrogels were synthesized with ACR and crosslinked at 5-20 mole % crosslink densities with PEGDA (degradable via hydrolysis) or 5 mole % BIS (non-degradable). Gelation was initiated with APS stabilized with TEMED and cured for 25 minutes or until solid.

When utilizing gels for enzyme activity studies, lactase enzyme was added just prior to gelation initiation. Thin films approximately 75 μm thick were fabricated by drop casting 30 μL of the solution onto activated coverslips. These films were washed in PBS for 3 hours then placed in 6-well plates with ONPG substrate. Conversion was measured through ONP production every 20 seconds for 10 minutes at $\lambda = 420 \text{ nm}$. This was repeated for 0.1, 0.2, 0.4, 1, and 10 mg/mL ONPG/PBS substrate concentrations. To determine retention of enzymatic activity within the biogels, kinetic studies were performed at $t = 3, 24, \text{ and } 48$ hours. Lineweaver-Burk plots were created to determine the Michaelis-Menton constant, K_m , and the maximum reaction velocity, V_{max} .

3.3.4.1 Storage Activity and Repeatability/Reliability of Production using Biogels

Kinetic studies were performed at $t = 3, 24, \text{ and } 48$ hours to determine retention of enzymatic activity within the gels. Lineweaver-Burk plots were created to

determine the Michaelis-Menton constant, K_m , and the maximum reaction velocity, V_{max} .

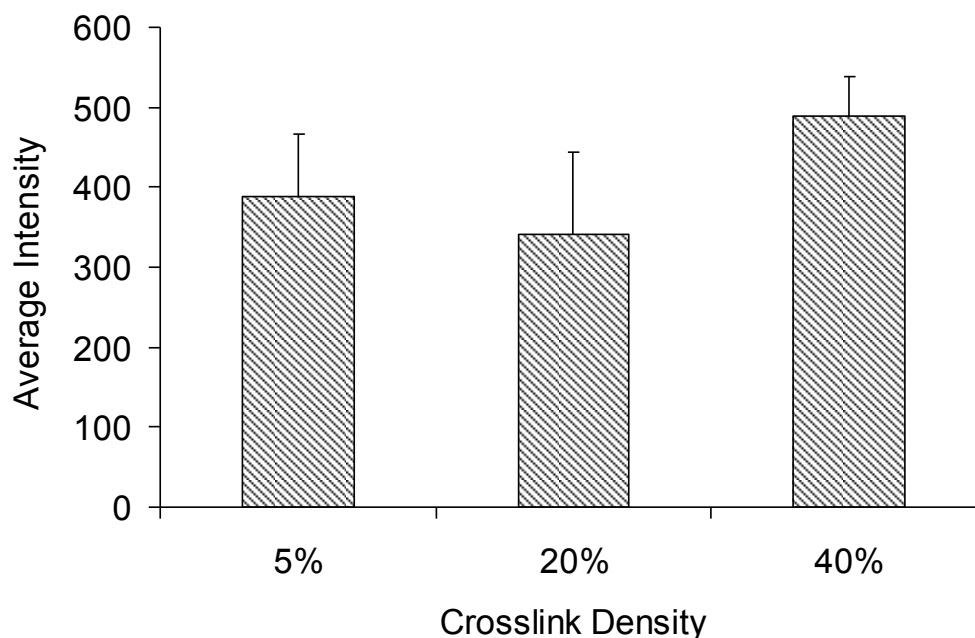
3.3.4.2 Preservation of Enzymes Entrapped in Biogels

Kinetic studies to determine the preservation of enzyme activity when challenged by an environmental pH change of 8 were performed directly after washing in PBS for 3 hours. At a pH of 8 a low amount of free enzyme in solution should remain active allowing for comparison with the fabricated biogels. This pH was chosen as it is also applicable for use in the charged monomer studies, allowing the AMPS (-) to remain highly deprotonated and the MAPTAC (+) to remain highly protonated. The samples were tested directly after the wash period and then the substrate media was removed. 200 μ l of 500 μ M NaOH was pipetted on top of the biogels and allowed to react for 1 minute before the subsequent addition of ONPG dissolved in PBS. Maintained activity is reported as a percentage of the maximum enzymatic velocity (V_{max}) of catalytic conversion of substrate into product.

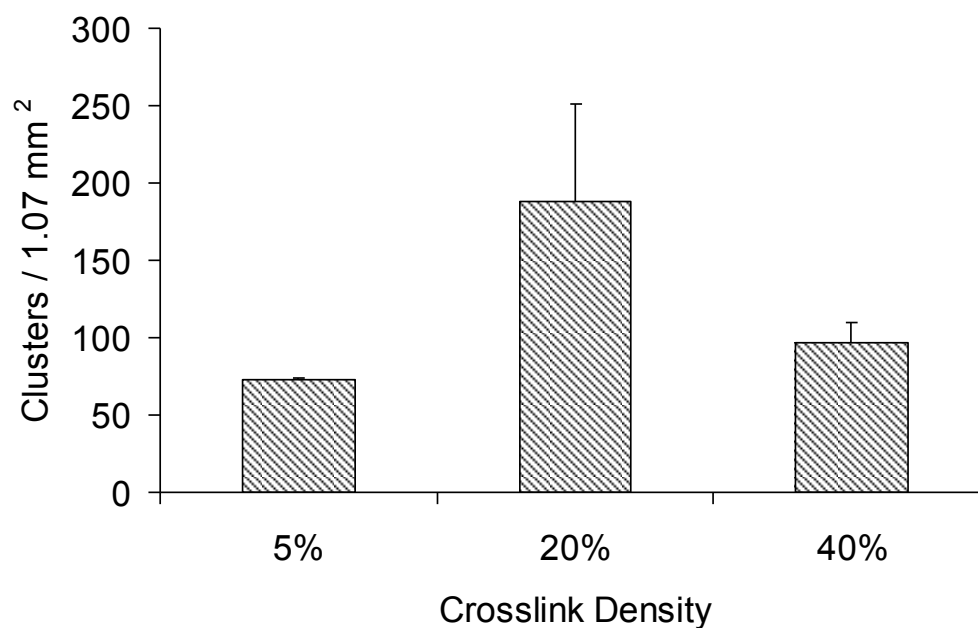
3.4 Results

3.4.1 Confocal Microscopy

Fluorescence images were taken and analyzed for gels with crosslink densities of 5, 20, and 40%. Three images were taken over a depth of 10 μ m in order to ensure that enzymes were entrapped within the network and not adsorbed to the surfaces. The depth images were compiled into a single image and analyzed using ImageJ to obtain average intensities and clustering. Each image obtained was for a standard 1.07 mm² area. Enzyme clusters were located and determined by bright spot analysis.



A



B

Figure 9. Confocal Imaging of Entrapped Enzyme

A) Enzyme distribution as measured through intensity analyzed using ImageJ software. Background intensity was determined on gels with no enzyme and subtracted out of the signal. Error is reported as standard error of the mean.

B) Measurement of clustering through the use of ImageJ to determine bright intensity segments related to groups of labeled enzymes within the gel matrices. The cutoff value in ImageJ was set to 50 to determine fluorescent clusters from the background. Blank gels of each crosslink density contained no bright spots. Error is reported as standard error of the mean.

The average intensity measured for all gels was equal, denoting that an equal amount of enzyme was entrapped within each gel regardless of crosslinker concentration as seen in Figure 9a. Blank, enzyme free, gels were tested to determine the background autofluorescence of fabricated ACR/PEGDA gels and subtracted from the fluorescence intensity of the biogels. The only statistical difference in average intensity was determined between the biogels, gels with active fluorescently labeled enzyme entrapped, and the blank gels, supporting the conclusion that equal amounts of enzyme were entrapped within each fabrication of the biogels..

Clustering data as depicted in Figure 9b shows a non-uniformity of enzyme/area. There was a large standard error related to the 20 mole % crosslinked data. To further understand if the areas of high intensity were actual enzyme clusters future work will endeavor to pre-cluster fluorescently labeled enzyme prior to entrapping them within the biogels. These studies will allow for better understanding of the data observed in Figure 9b. It is believed that the increase in crosslinks per volume of gel would force the enzyme to cluster into small groups prior to complete polymerization, instead of being distributed evenly within the biogel. In order to prove such a theory much more data would be required and thus it was not investigated further. The overall conclusions of these experiments was that enzyme is entrapped non-uniformly within the biogel matrix.

3.4.2 Positive Control Studies

3.4.2.1 Solution and Chemical Fixation

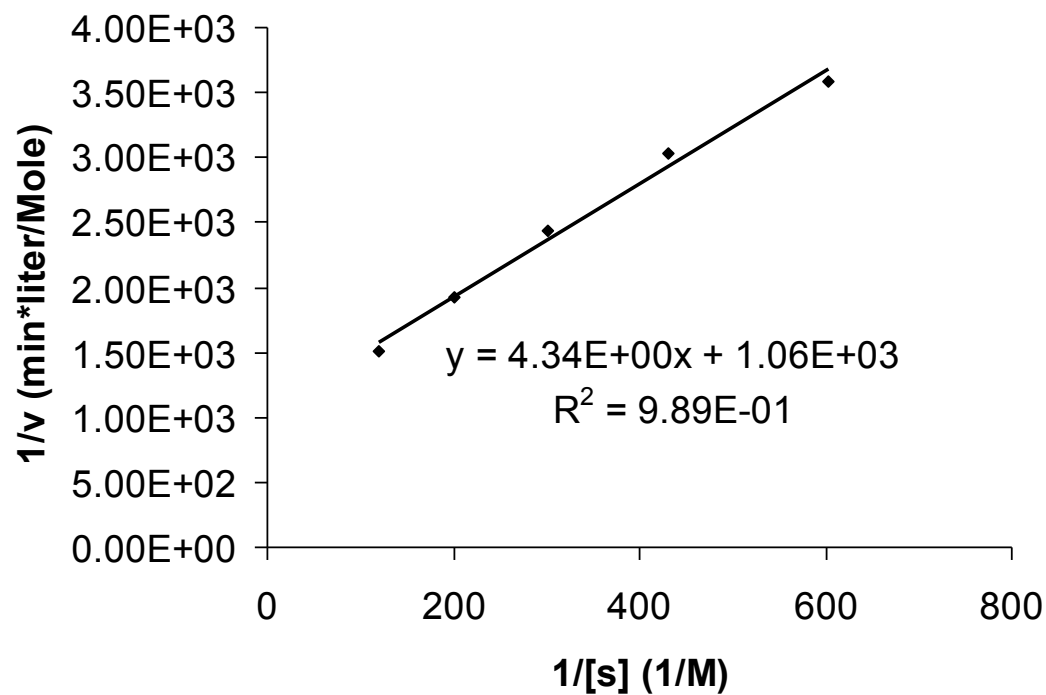
Solution based kinetics were determined for PBS diluted lactase matching quantities utilized in biogel studies. To determine the solution based activity retention over extended periods of time, samples were “aged” by diluting purchased lactase with PBS and storing these diluted samples at 4 °C in PBS for 2, 24, and 48 hours as well as 8 and 15 days. The parameters, V_{\max} ($\mu\text{M/L/min}$) and K_m (μM), were ascertained through the application of Lineweaver-Burke plots of the aged enzyme solution based on conversion studies at 2, 24, and 48 hours as well as 8 and 15 days. The maximum velocity of conversion, V_{\max} , determined at 2 hours, was $1520 \pm 180 \mu\text{M/L/min}$. It decreased as the sample was aged to the eighth day to $1070 \pm 200 \mu\text{M/L/min}$. Increased aging time had an inverse relationship to V_{\max} indicating that the enzyme becomes less effective due to deterioration over time. K_m , an indication of the enzyme pocket’s binding efficiency should not change and as expected, K_m remained relatively unchanged at $2600 \pm 260 \mu\text{M}$. Tests with and without activated glass slides showed no significant differences.

Chemical fixation enzyme kinetic parameters were determined using lactase crosslinked onto glass coverslips and washed in PBS for 2 hours. The determined $V_{\max} = 230 \pm 140 \mu\text{M/L/min}$ and $K_m = 2190 \pm 420 \mu\text{M}$, related only to enzyme adsorbed and chemically fixed to the glass slide. As expected these values were less than solution based enzymatic activity, as much of the enzyme did not crosslink onto the glutaraldehyde activated slide and was washed away.

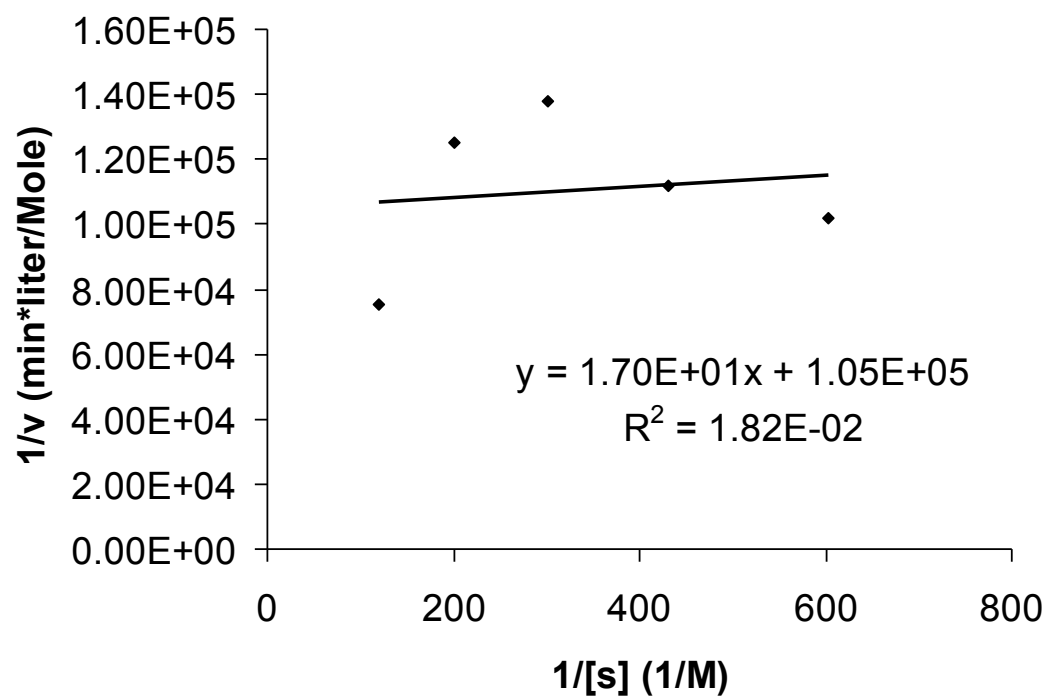
3.4.2.2 Enzyme Diffusion out of Biogel

Entrapment conversion studies are dependent on the assumption that active enzyme loss is not prominent past the first wash cycle. Results presented in this section prove this to be the case. Figure 10 represents the obtained kinetic values from Lineweaver-Burke plots of a 30% PEGDA crosslinked biogels, the initial wash and a subsequent wash 20 minutes later. The initial wash, containing free enzyme from the entrapment method, Figure 10a, showed a measureable amount of enzyme leading to the conversion of ONPG to ONP. The second wash 20 minutes later, shown in Figure 10b, showed no measurable kinetic parameters from the obtained Lineweaver-Burke plot indicating that no appreciable amount of enzyme had been washed away with the second wash. Similar results were seen in comparatively long duration wash studies of 24 hours proving that relatively low to no leaching of active enzyme into the PBS storage media occurred. Figure 10c showed maintained biogel functionality, shown through measurable conversion kinetics, after removing the first and second washes.

A



B



C

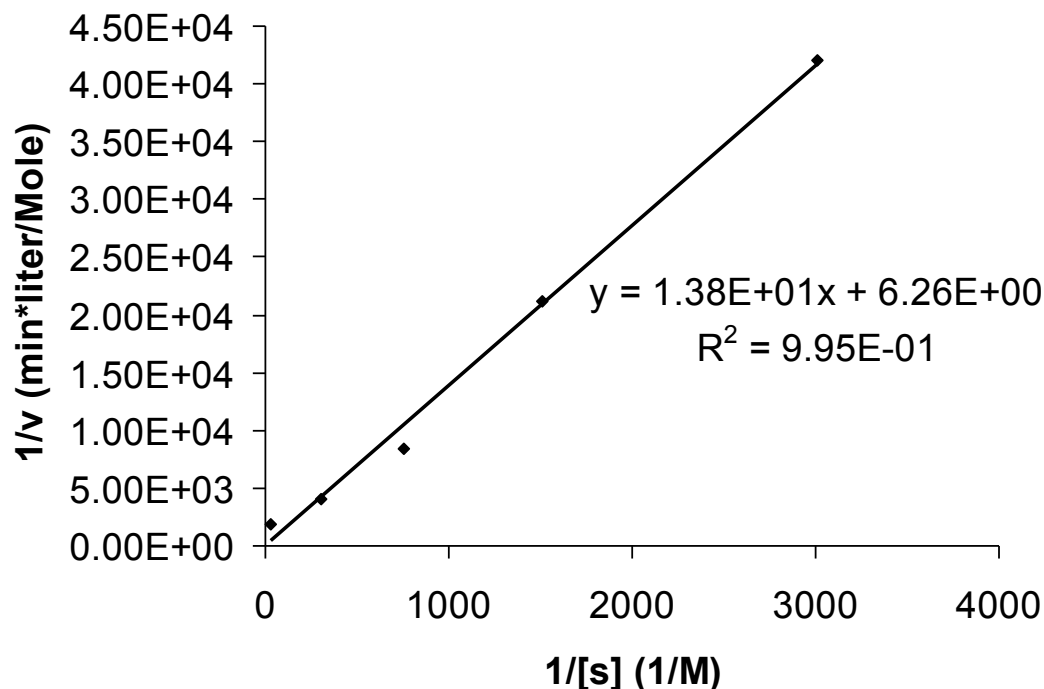


Figure 10. Lineweaver-Burke plots of Enzyme Diffusion

Lineweaver-Burke plots of PBS wash buffer removed from 30% PEGDA crosslinked gels where $1/[s]$ in 1/M is the concentration of ONPG substrate and $1/v$ in min*liter/Mole is $1/(\text{the velocity of enzymatic conversion})$.

A) First wash fluid at 3 hours containing initial free enzyme and unreacted reagents.

B) 20 minutes later, 2nd wash fluid containing leached enzyme from the drop cast biogel, proves no active enzyme leached into solution.

C) 30% PEGDA crosslinked biogel after 2nd wash proving maintained enzyme entrapment within the network.

From the study shown in Figure 10, V_{\max} of the first wash fluid and the biogel were compared to show initial loss of enzyme due to this wash. V_{\max} of biogel/wash buffer showed a reduction in active enzyme units equal to 27%. Solution based positive controls utilize this reduction to correct for enzyme that would have been lost in the wash cycle if washing had been possible.

3.4.2.3 Enzyme Entrapped in Alginate Hydrogels

To compare the efficiency of maintaining enzymatic activity, the fabricated ACR gels crosslinked with PEGDA were judged against the biopolymer alginate. Lactase was entrapped in 1, 2, or 3 % weight per volume alginate gels and used to determine K_m and V_{max} . As can be seen in Figure 11, no measurable levels of activity were maintained post-entrapment were determined using the Lineweaver-Burke method. Alginate gels also deteriorated in the aqueous ONPG dissolved in PBS as monovalent cations replaced calcium in the gel formation as seen in Figure 12. This obstacle was alleviated by dissolving ONPG in a 50 mM $CaCl_2$ solution. This did nothing to improve the activity of the entrapped enzyme. Figure 13 shows the slight color change is contained within the alginate particle and does not diffuse into the media. These results indicate the viability and superiority of ACR/PEGDA biogel method for use in enzyme entrapment and protection.

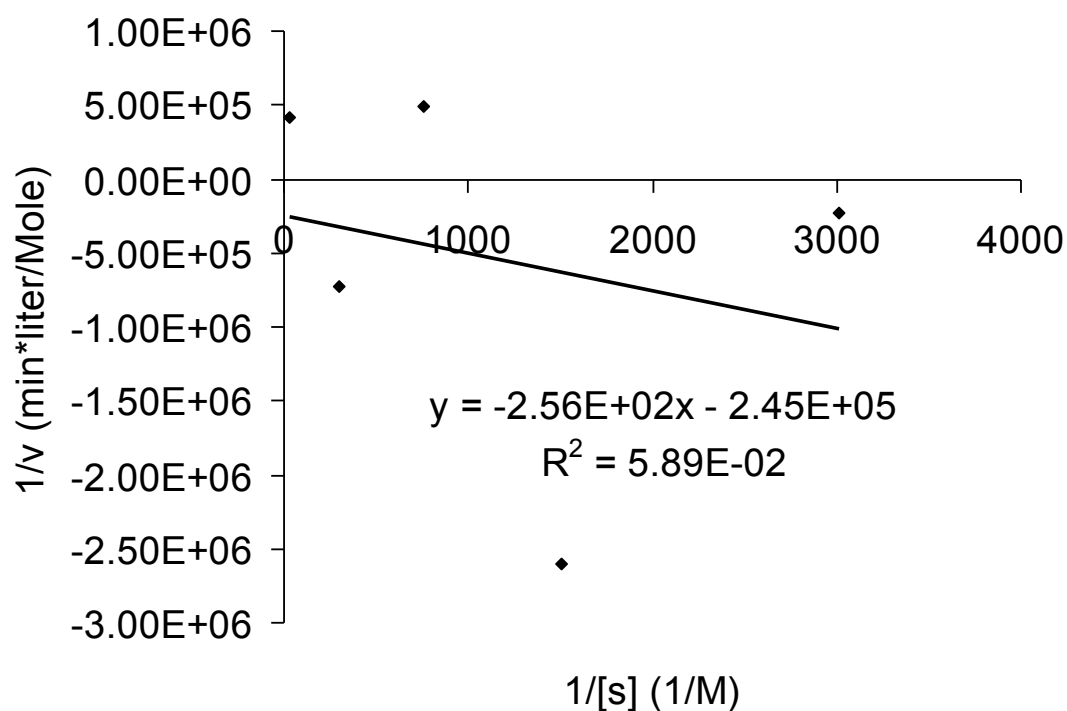


Figure 11. Lineweaver-Burke plot of Alginate Entrapment of Enzyme

Lineweaver-Burke plot of enzyme entrapped within 2 % (w/v) alginate gels showing no retention of activity. Where $1/[s]$ in 1/M is the concentration of ONPG substrate and $1/v$ in min*liter/Mole is $1/(\text{the velocity of enzymatic conversion})$.

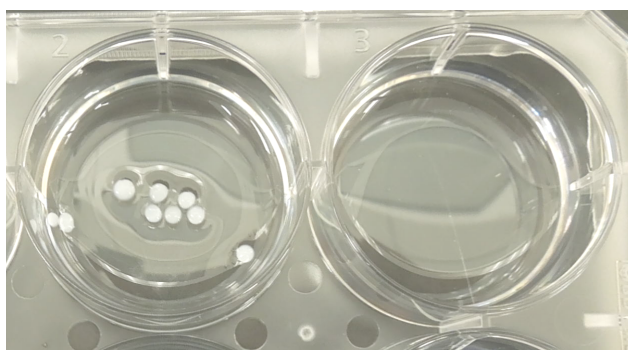


Figure 12. Alginate Fabrication and Dissolution in PBS

2 weight/volume % alginate gels created by drop pipetting into 50mM calcium chloride solution. Beads made in the well to the left and were subsequently placed in the well to the right containing PBS. Complete dissolution of the gels was seen in 5-10 minutes.

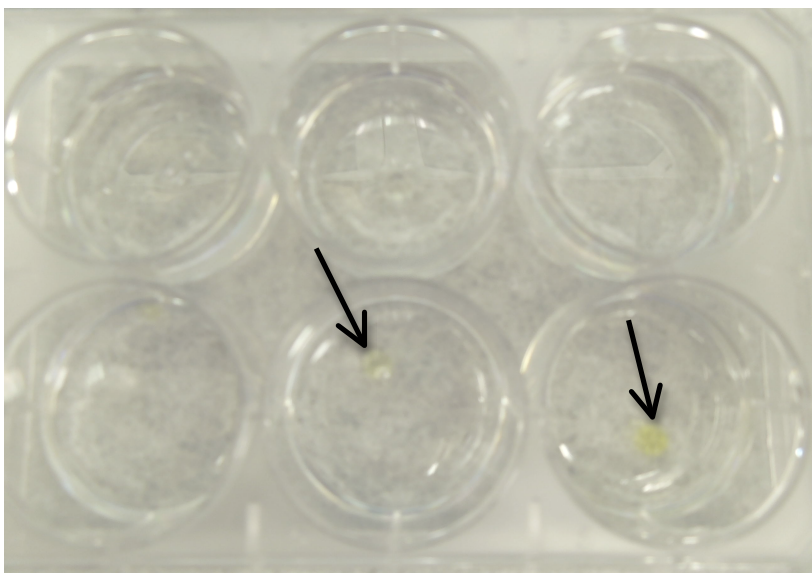
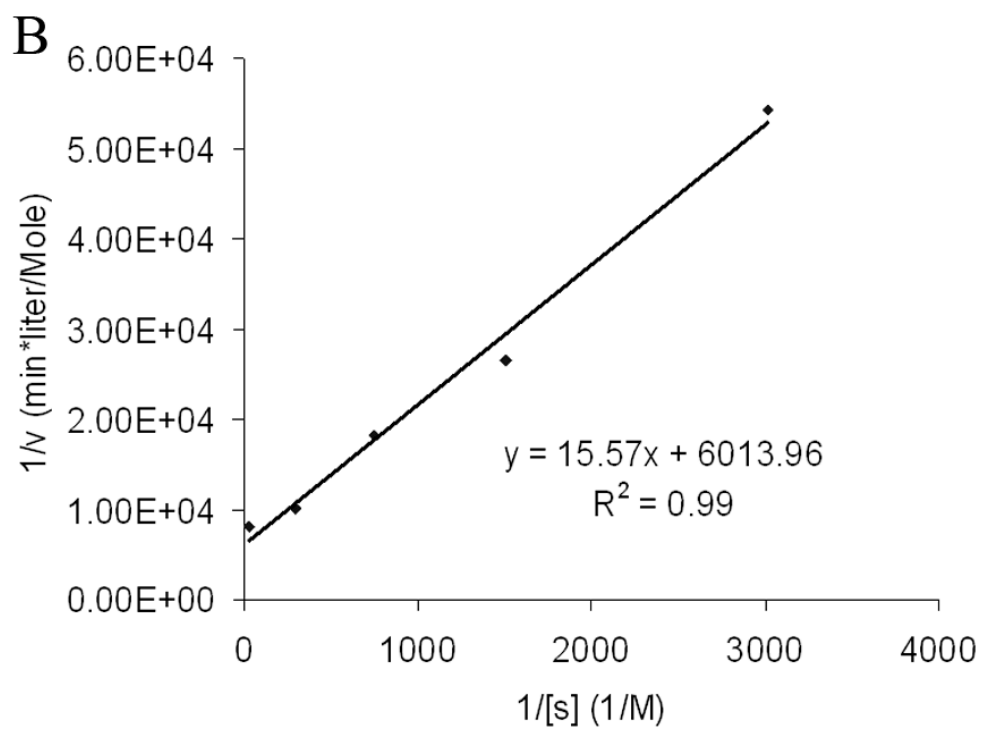
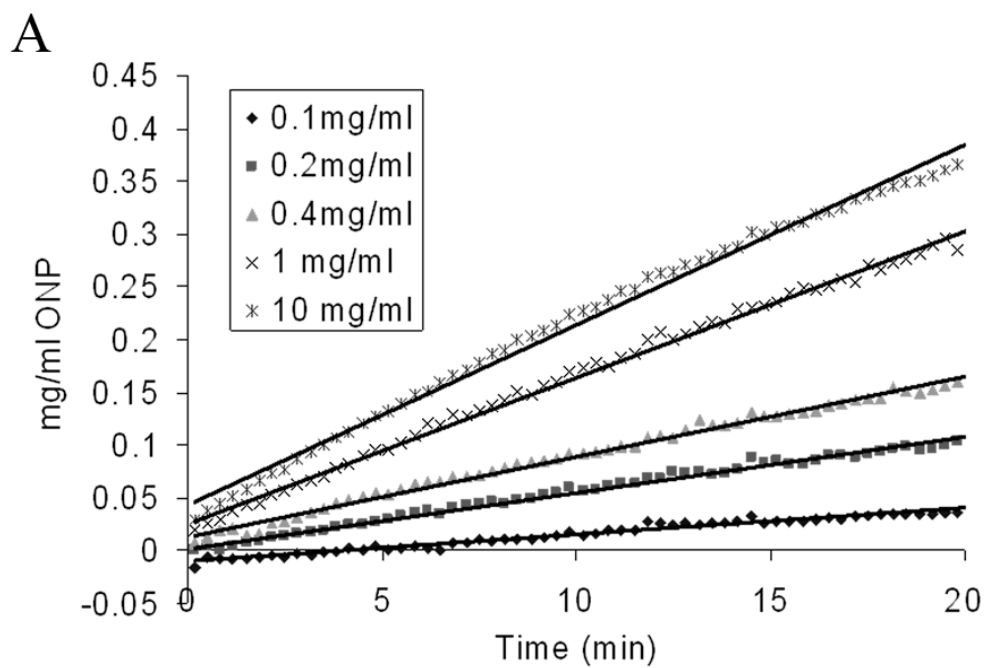


Figure 13. Alginate Biogels Converting ONPG into ONP

2 % weight/volume alginate biogels converting ONPG to ONP. Yellowing shows conversion directly in the bead, however there is no diffusion of the ONP out of the biogel into the surrounding fluid.

3.4.3 Enzyme Activity

Lactase enzyme was entrapped within the following biogel network: 5 mole % BIS crosslinked, 5, 7, 10, 13, 20, 25, 30, 35, and 40 mole % PEGDA crosslinked as discussed in the methods section. After washing, these gels were tested for enzymatic activity through ONPG to ONP conversion studies. Figure 14a shows a typical time-lapse kinetic conversion curve of BIS and PEGDA crosslinked gels, whereas Figure 14b shows the resulting constructed Lineweaver-Burke plot obtained from the respective conversion graph. The parameters V_{\max} and K_m were calculated using these plots.



C

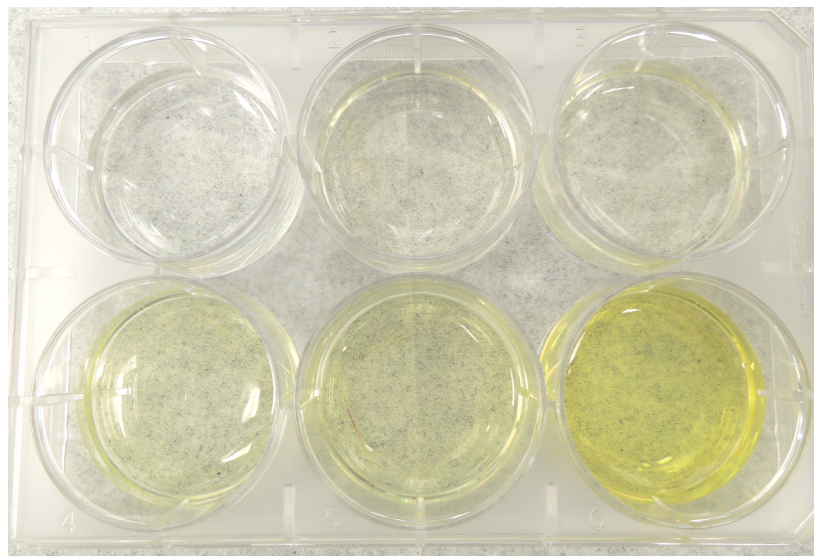


Figure 14. Lineweaver-Burke plot: Experimental Setup and Analysis

A) 5% BIS crosslinked gel substrate ONPG conversion into product ONP at 3 hours post-entrapment of various concentrations of substrate ONPG.

B) Lineweaver-Burke plot of 5% BIS crosslinked gels at 3 hours post-entrapment, where $1/[s]$ in $1/M$ is the concentration of ONPG substrate and $1/v$ in $\text{min} \cdot \text{liter}/\text{Mole}$ is $1/(\text{the velocity of enzymatic conversion, seen as the slope in Figure 4a})$.

C) Representative 6-well conversion study plate used to obtain ONP concentrations at $\lambda = 420 \text{ nm}$. Blank hydrogel in well 1 and biogels in wells 2-6 are placed at the bottom of each well and 10, 0.1, 0.2, 0.4, 1, and 10 mg/mL ONPG/PBS substrate is introduced allowing for the determination of V_{max} and K_m .

3.4.3.1 Storage Activity and Repeatability/Reliability of Production using Biogels

After washing, these gels were tested for enzymatic activity through ONPG to ONP conversion studies. The parameters V_{max} and K_m were derived for each synthesized gel at various time points including 3, 24, and 48 hours post-entrapment. Representative data are reported in Figure 15.

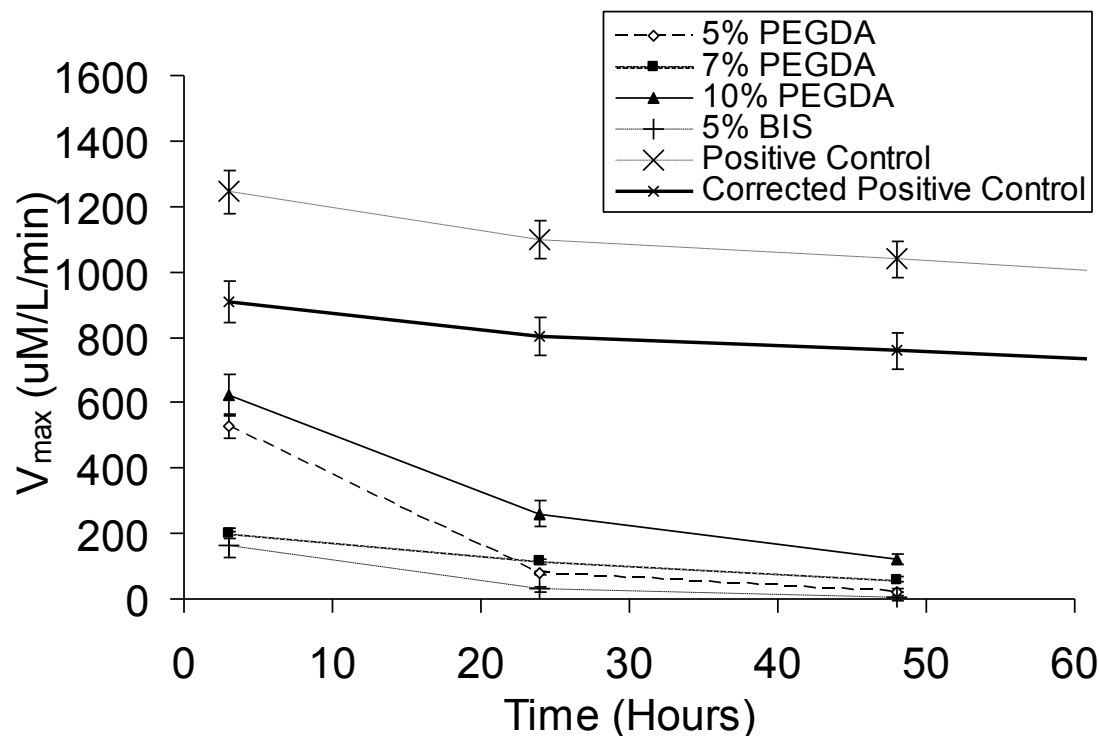


Figure 15. V_{max} over a Two Day Period: Low Crosslink Density Studies

Enzymatic V_{max} in ($\mu\text{M/L/min}$) low crosslink density gel compositions. PEGDA gels outperformed BIS gels. Increasing PEGDA crosslink density enhanced retention up to 10% crosslink density. Error reported as standard error of the mean.

Figure 15 shows initial responses to entrapment decreased the V_{max} of approximately 40% from free enzyme, depending on the density and type of crosslinker utilized for the biogel. This initial loss of activity was due to the gelation process and resulting loss of enzyme. The majority of the initial enzyme substrate (ONPG) to product (ONP) velocity loss is due to the loss of active enzyme into the initial wash buffer. This buffer contained enzyme that remained free throughout the biogel fabrication process as well as any unreacted reagents. The remainder of lost activity is assumed to be a byproduct of the free radical initiator, APS. APS is a strong oxidizer that will react with any molecules, not just the monomer and crosslinker in solution. The chemical reaction between APS and the enzyme leads to

its subsequent deactivation. BIS crosslinked biogels maintained the least activity upon initial entrapment when compared with PEGDA crosslinked biogels. It is thought that this phenomenon resulted from the additional protection provided by the hydrolyzable PEG linkages of the PEGDA biogels. These bonds allow for extra molecular sites for APS to be consumed before coming into contact with enzyme. To verify this assumption, Figure 15 also shows increased density of PEGDA crosslinks increased V_{\max} retention over 48 hour time trials.

PEGDA crosslink densities above 10% began to show a decrease in V_{\max} both initially and retention over time was diminished as can be seen in Figure 16. It is assumed that PEGDA crosslinker creates a more habitable environment for the enzyme, allowing for increased retention in activity until steric hindrances caused by dense crosslinks effect the enzyme's ability to change its conformation.

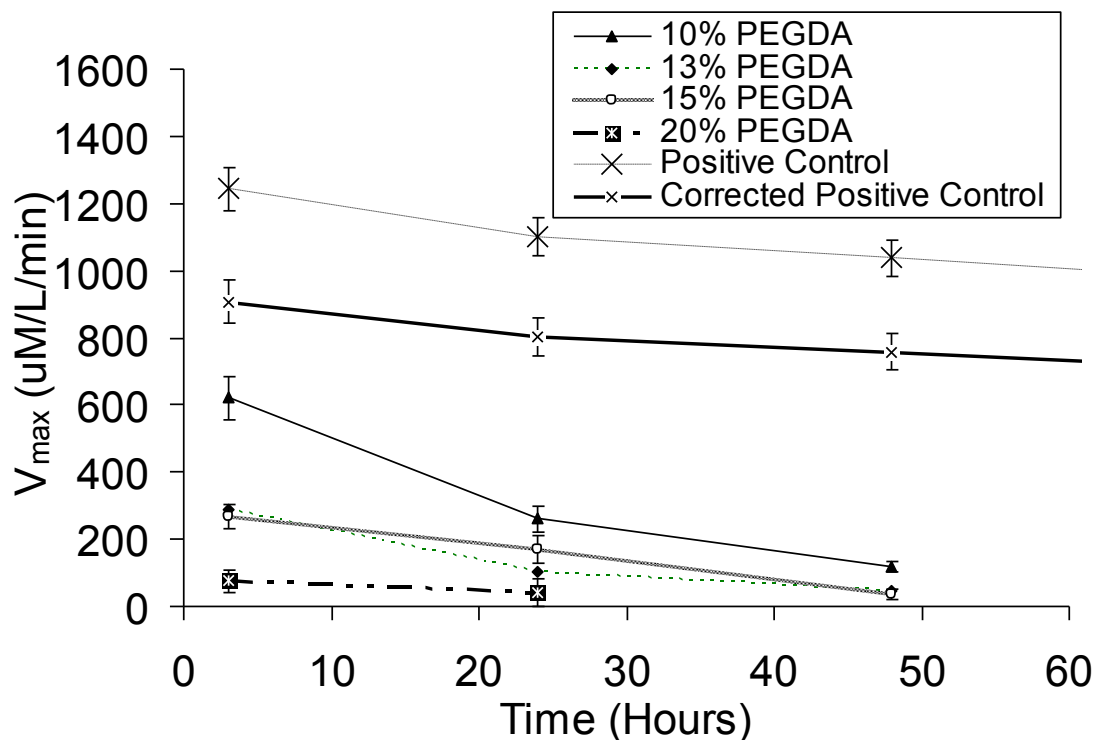


Figure 16. V_{\max} over a Two Day Period: High Crosslink Density Studies

Enzymatic V_{\max} in ($\mu\text{M/L/min}$) high crosslink density gel compositions. Decreased V_{\max} retention is shown in gels with greater than 10% crosslink density. Error reported as standard error of the mean.

The K_m was recorded for all experiments and resulted in $K_m = 3070 \pm 1710$ μM , as seen in Figure 17. Ideally, K_m should remain constant through the use of the same enzyme and same batch. Variation was most likely due to affinity changes caused by random enzymatic conformational changes over time and through the entrapment procedure. No commonalities or trends were seen between BIS or PEGDA crosslinked gels nor through variations of crosslink density indicating that K_m was not altered due to specific testing methods, only that it was altered due to random enzymatic morphological changes.

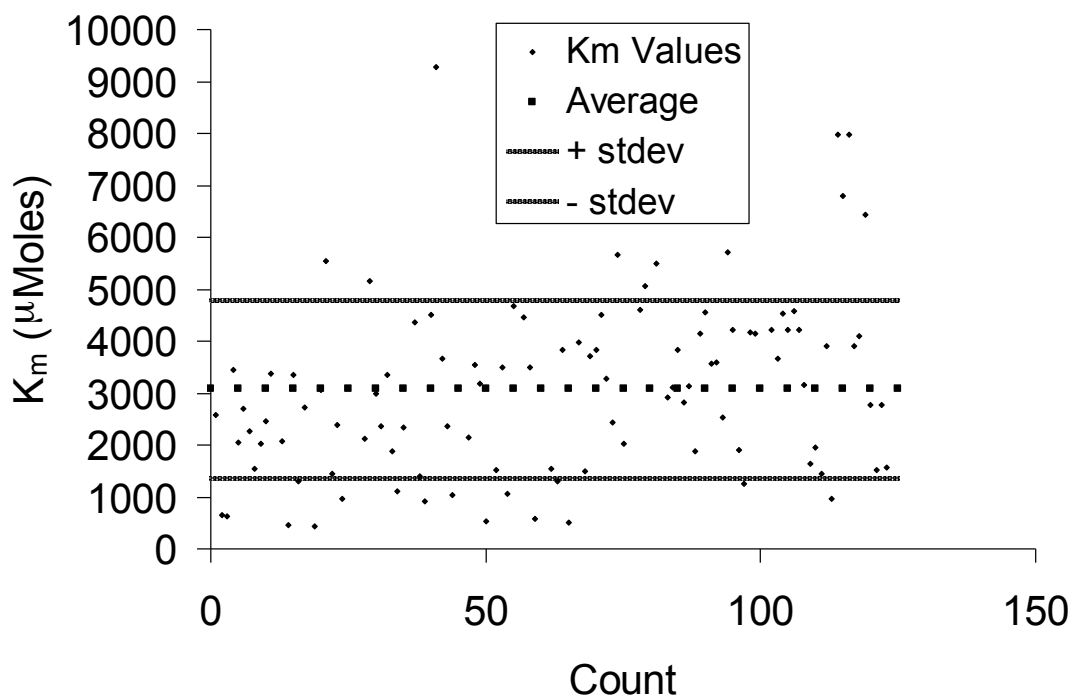


Figure 17. Calculated K_m over all Studies

Enzymatic K_m in (μM). No correlation was found between treatments of samples to account for the large error in this value. Variation is assumed to be due to affinity changes of the catalytic pocket due to storage and the free radical gelation process.

3.4.3.2 Preservation of Enzymes Entrapped in Biogels

Table 8 compares retention of activity for entrapped enzymes to control studies. The enzyme activity was tested and then compared to the activity after the pH was raised from 7.4 to 8. Increasing the crosslink density increased the enzyme stability through the pH challenge as indicated by the increased retention of V_{\max} . It is presumed that the PEGDA bonds absorb a number of the OH^- molecules leading to partial hydrolysis of the PEGDA crosslinker and stabilizing the pH toward more favorable levels. The control in this study is not corrected to enzyme loss during the wash cycle because the wash out enzyme would be the same both before and after the challenge of pH 8, thus making it an unnecessary algebraic step.

Table 8: V_{\max} retention of PEGDA crosslinked biogels when exposed to NaOH

	V_{\max} Retention	Standard Deviation
30% PEGDA	48%	$\pm 18\%$
35% PEGDA	85%	$\pm 4\%$
40% PEGDA	91%	$\pm 10\%$
Control	23%	$\pm 8\%$

Retention is reported as a percentage of normal conditions vs. post 1 minute application of NaOH solution pH 8.

3.5 Conclusions

This work demonstrated an effective entrapment method that preserves enzyme activity within a favorable environment and resists activity reduction due to a change in pH of the system. Lactase entrapped within ACR/BIS showed poor retention of initial and extended V_{\max} retention as compared to when entrapped in ACR/PEGDA hydrogel matrices. The crosslinker molecule PEGDA acted to protect the enzyme from overall structural degradation and as PEGDA crosslink density increased between 5-10%, enzymatic retention increased. It is expected that crosslink densities of 15-40% decreased enzymatic retention due to steric hindrance of the enzyme and decreased diffusion of substrate to the active sites of the enzyme. This entrapment method shows marked improvement upon entrapment compared to alginate gels and shows promise for use in on-demand applications.

Chapter 4: Biogel Characterization with Positive and Negative Monomer Moieties

4.1 Objectives

The two main objectives to characterize the effects of positive and negative monomer moieties within the biogel were: 1) determine the stabilizing effects of positive and negative charge density within the matrix on the entrapped enzyme by studying production repeatability over a two day storage time, and 2) characterize the protection of the enzyme using positively or negatively charged monomers when the biogels are environmentally stressed to a pH of 8.

4.2 Introduction

Within entrapment techniques, other methods to increase enzyme activity retention are to create favorable cavities surrounding the enzyme. This matrix can be created through the addition of charged or hydrophobic moieties. Optimizing these electrostatic interactions is a simple and effective way to improve enzyme stability without altering the core folding and active sites (13). Increased interactions create desired cavities while not impinging natural functions (23, 28)

4.3 Methods

4.3.1 Materials

Acrylamide (ACR), N,N-dimethylacrylamide (NDMA), [3-(methacryloylamino) propyl]trimethylammonium chloride (MAPTAC) , 2-

acrylamido-2methyl-1-propanesulfonic acid sodium (AMPS), *N,N'*-methylenebisacrylamide (BIS), poly(ethylene glycol)diacrylate ($M_n = 700$ PEGDA), ammonium persulfate (APS), *N,N,N',N'*-tetramethylethylenediamine (TEMED), ortho-nitrophenyl- β -D-galactopyranoside (ONPG), phosphate buffered saline (PBS) and β -galactosidase (lactase, 476kDa) from *Kluyveromyces lactis* were purchased from Sigma Aldrich and were used as received except for MAPTAC and PEGDA, where the chemicals were first filtered through an inhibitor removal column prior to application. A plate reader (SpectraMax(R) M5, from Molecular Devices) set on 6 well plate and absorbance at $\lambda = 420$ nm was employed to measure the bound enzymatic degradation of ONPG into ONP every 20 seconds for 10 minutes.

4.3.2 Positive Control Studies

4.3.2.1 Solution Kinetics

As an enzyme ages, the amount of active enzyme per volume in the purchased sample decreases, therefore it was necessary to perform positive controls of enzyme solution kinetics as a reference point for the experimental entrapment and protection procedures. Positive controls were performed in a similar manner as described in section 3.4.2.1 and consisted of lactase enzyme diluted with PBS to match quantities utilized in biogel studies. Samples were refrigerated at 4 °C in PBS for 2, 24, and 48 hours to determine the solution based activity retention over two days time. At the indicated time point, ONPG in concentrations of 0.1, 0.2, 0.4, 1, and 10 mg/mL PBS, was introduced to the enzyme in solution and conversion of ONPG to ONP was measured at $\lambda = 420$. These conversion results were then used in Lineweaver-Burke

plots to determine V_{\max} and K_m . The calculated conversion rates were the solution based free enzyme Michaelis–Menton constants.

4.3.3 Enzyme Activity

Two variations of these experiments were tested: 1) the storage and conversion effects of added monomer moieties to the hydrogel matrix over a two day study, and 2) the ability of the matrix to protect enzymes from environmental deviations in pH from 7 to 8.

4.3.3.1 Storage Activity and Repeatability/Reliability of Production using Biogels

The storage effects were determined by fabricating 10 mole % PEGDA biogels with 0, 5, and 10 mole % MAPTAC (+) or AMPS (-) monomer moieties. Five thin film biogels and one blank, enzyme free biogel also known as a hydrogel, of each species were fabricated by drop casting 30 μL of the desired mixture and allowing them to set for 10 minutes. These were then placed in 6 well plates and incubated in a PBS solution for 2 hours to remove excess, unreacted reagents. Kinetic parameters were determined by introducing of 0.1, 0.2, 0.4, 1, and 10 mg/mL ONPG in PBS substrate to the biogels and recording the absorbance, which directly correlates to enzymatic conversion of ONPG to ONP, at $\lambda = 420$ over 10 minutes. The absorbance directly correlates to enzymatic conversion of ONPG to ONP. Gels were then stored in PBS for 24 hours, tested for enzymatic activity and the ability for biogel repeatable synthesis, stored for another 24 hours (total of 48 hours) and tested a final time. Lineweaver–Burke plots were constructed to find V_{\max} and K_m at each of the time points: 2, 24, and 48 hours.

4.3.3.2 Environmental Protection of Enzymes Entrapped in Biogels

The ability of the matrix to protect the enzyme from overall degradation in perturbed environments of pH 8 were determined through the fabrication of 20 mole % PEGDA crosslinked biogels with 0, 5, 15, or 20 mole % AMPS (-) or MAPTAC (+) monomer moieties. This pH is applicable for use in such charged monomer studies, allowing the AMPS (-) to remain highly deprotonated, with a pKa of 2 and the MAPTAC (+) to remain highly protonated, with a pKa of 12. Again, five thin film biogels and one blank, enzyme free, hydrogel of each variety of gel were created, incubated for 2 hours to remove unreacted reagents, and tested in the 0.1, 0.2, 0.4, 1, and 10 mg/mL ONPG in PBS substrate for conversion to obtain V_{\max} and K_m . Directly afterwards, the biogels were challenged with pH 8 NaOH solution or pH 8 borate buffer solution for one minute. Kinetic parameters were determined through the biogel conversion after the environmental test in order to compare the biogels' V_{\max} retention.

4.4 Results

4.4.1 Positive Control Studies

4.4.1.1 Solution Kinetics

Solution based enzymatic activity parameter V_{\max} , as determined through Lineweaver-Burke plots of conversion studies at 2, 24, and 48 hours, are displayed in Figure 16. The positive control values provided a reference point for the monomer moiety biogel entrapment and protection procedures. As expected, solution based kinetics have the highest maximum reaction velocity as compared to the biogels.

Enzyme may lose its activity during the entrapment procedure as the radical initiator APS can react with enzymes that it comes into contact with, altering the protein's conformation and denaturing them. Entrapment within the matrix may also hinder natural conformational changes making it difficult or impossible for enzymes to catalyze substrate at high crosslink densities.

4.4.2 Enzyme Activity

4.4.2.1 Storage Activity and Repeatability/Reliability of Production using Biogels

The storage effects on V_{\max} of added monomer moieties to the hydrogel matrix are shown in Figure 18. Kinetic parameters were determined for 10 mole % PEGDA biogels with 0, 5, and 10 mole % MAPTAC (+) or AMPS (-) monomer moieties at 2, 24 and 48 hour post-entrapment. High levels of AMPS (-) induced improved V_{\max} retention over time as compared to all other biogels, including ACR/PEGDA biogels. It is thought that the high ratio of negatively charged groups to enzyme stabilized the protein, allowing it to remain unperturbed within the gel construct over the two day study. The initial level of activity, though 40% reduced from the corrected positive control, did show a slight improvement over ACR/PEGDA gels without monomer moiety additions. Low levels of AMPS (-) monomer additions had poor initial V_{\max} and poor retention of this velocity over the two day studies. One explanation is that the density of these charged groups is not high enough to stabilize the protein, only enough to increase swelling through coulombic repulsion, possibly enough to create cavities large enough for the enzymes to move and become denatured. Similarly, at the tested 10% crosslink density, positive monomer additions reduced the initial 2 hour maximum velocities as

compared to ACR/PEGDA only gels. The retention of activity over the two day study was slightly improved compared to the ACR/PEGDA gels, but no conclusions can be made from this small variation.

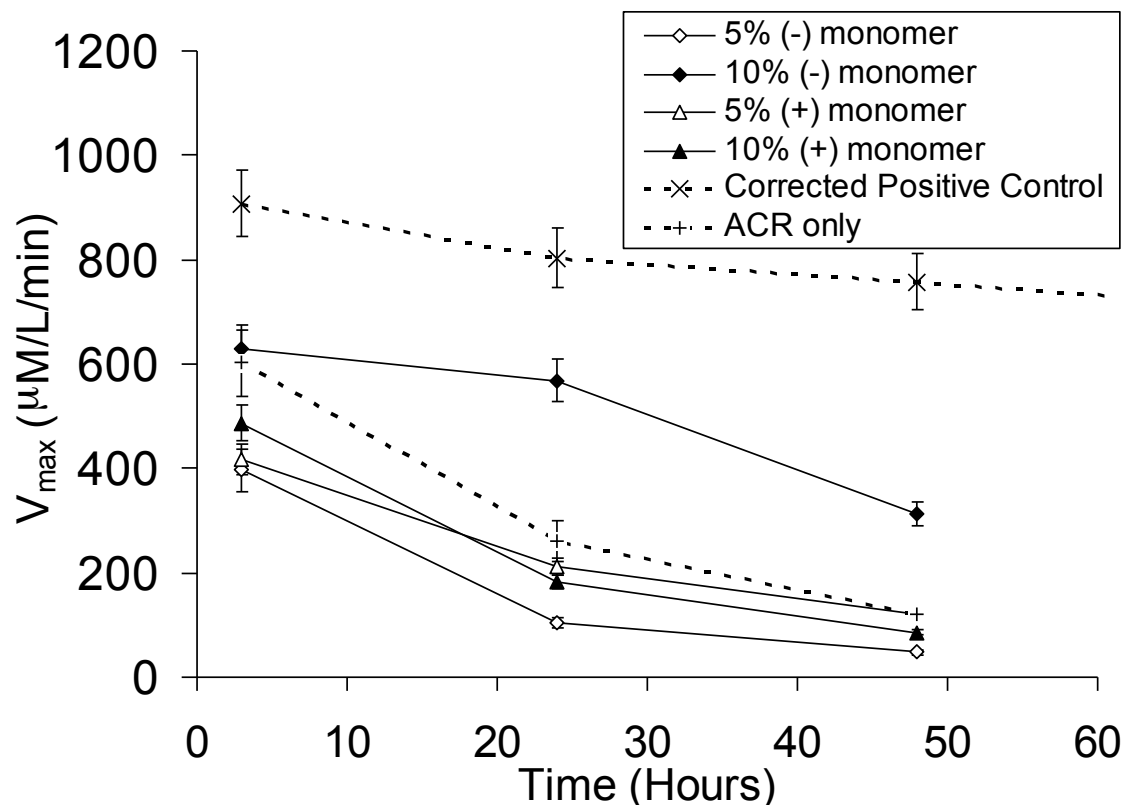


Figure 18. Calculated V_{\max} Two Day Study: Charged Matrices

V_{\max} of 10 mole % PEGDA crosslinked hydrogels with 0, 5, or 10 mole % of MAPTAC (+) or AMPS (-) monomer. Positive control demonstrates solution kinetics. High, 10 mole % AMPS (-) monomer concentrations yielded the best storage and most reliable product molecule formation over the two day study. Error reported as standard error of the mean.

At this time and in the current stage of development of these biogels, prolonged activity past a two day study yields low V_{\max} retention. Future studies can focus on increasing the initial amount of entrapped enzyme in order to prolong biogel activity and determine long term retention.

4.4.2.2 Environmental Protection of Enzymes Entrapped in Biogels

The results from the environmental biogel experiments are shown in Tables 9 and 10. Two different crosslink densities, 5 and 20 mole % (Tables 9 and 10, respectively) were tested for protection with 0, 5, 10, 15 or 20 mole % MAPTAC (+) or AMPS (-) monomer moieties against two different environmental alteration solutions: NaOH or borate buffer saline (BBS) pH 8 (Tables 9 and 10, respectively). Overall, higher crosslink density gels did better to protect the enzyme as reported earlier in this thesis. To negate the protection caused by high crosslink density, 5 mole % PEGDA crosslinked gels were tested with the addition of MAPTAC (+) or AMPS (-) monomer moieties with the environmental challenge media, 500 μ M NaOH at pH 8. At this pH AMPS (-) remains highly deprotonated, and MAPTAC (+) remains highly protonated.

As seen in Table 9, the addition of MAPTAC (+) monomer had little to no effect on the retention of the velocity of enzymatic conversion of substrate into product. AMPS (-) however, showed an increase in protection with small amounts of the negatively charged monomer. It is assumed that the low density of negatively charged matrix monomers aided in deterring the adsorption of free hydroxyl groups to the enzymes within the biogel. Increased charge shielding occurring at high same charge density increases swelling allowing for the denaturing hydroxyl groups to reach the entrapped enzyme. High levels of AMPS (-) reduced the preservation of activity because it increased swelling and absorbance of OH⁻ groups. The hydroxyls within the swollen matrix can then come into contact with the enzyme denaturing them.

Table 9: V_{\max} retention of biogels challenged with NaOH

% of (+ or -) monomer	V_{\max} retention after NaOH introduction
10 (+)	51%
5 (+)	56%
0 (+ nor -)	51%
5 (-)	81%
10 (-)	20%

Table 10 reports V_{\max} retention at a higher crosslink density, 20 mole % PEGDA, with 0, 5, 10, 15 or 20 mole % MAPTAC (+) or AMPS (-) monomer moieties tested with BBS pH 8 as the degradation agent. Low levels of MAPTAC (+) increased retention of activity. It is presumed that the positive charge on the monomer associates with the negatively charged ions within the buffer to shield the enzyme from the denaturizing effects. Again, high levels of MAPTAC (+) decreased activity retention due to increased swelling leading to large cavities where the enzyme can come into contact with the BBS, denaturing the enzyme. Dissimilar from other reported results, increased AMPS (-) correlated to an increase in V_{\max} retention when the biogel was challenged with BBS. The negative charges within the matrix construct effectively reduce the amount of negatively charged ions from being adsorbed into the biogel, efficiently protecting the enzyme from this denaturation media.

Table 10: V_{\max} retention of biogels challenged with BBS

% of (+ or -) monomer	V_{\max} retention	Standard Deviation
20 (+)	61%	11%
15 (+)	69%	19%
10 (+)	48%	4%
5 (+)	67%	7%
0 (+ nor -)	52%	11%
5 (-)	53%	17%
10 (-)	58%	9%
15 (-)	64%	13%
20 (-)	75%	3%

4.5 Conclusions

This chapter determined that high, 10 mole %, AMPS (-) monomer concentrations yielded the best storage and most reliable product molecule formation over the two day study. Enzyme activity as determined through the retention of the maximum velocity of ONPG conversion into ONP was tested in two denaturation solutions of pH 8, NaOH and BBS. The addition of MAPTAC (+) monomer had little effect on preservation in NaOH solution, and small amounts of MAPTAC (+) increased V_{\max} retention in BBS. Most interesting is the positive correlation of AMPS (-) monomer concentration to V_{\max} retention when the biogels were tested with BBS. It is expected that the negative charges within the matrix effectively reduce the amount of negatively charged ions from being adsorbed, efficiently protecting the enzyme from this denaturation media.

Chapter 5: Overall Conclusions and Future Directions

The findings of this research can be applied to the enzymatic generation of desired biomolecules which are otherwise difficult to manufacture without the need for purification. By greatly reducing the need of a purification step, biomolecules can be produced at a more cost effective rate for the treatment of many diseases and in development strategies for diagnosis and vaccine development. The biogels fabricated show high enzymatic velocity retention compared to solution based kinetics when challenged to an increased pH of 8. This research holds the potential to increase enzymatic lifetime and allow for sustained reliable conversion of small molecules.

5.1 Synthesis and Characterization of Hydrogels

The material properties determined within this work have been related to the biogel activity. All fabricated hydrogels including: ACR/BIS, ACR/PEGDA, ACR/AMPS/PEGDA and ACR/MAPTAC/PEGDA showed Fickian swelling in PBS media. PEGDA crosslinked gels swelled more than BIS crosslinked gels, especially at high crosslink densities. Increased crosslink density decreased the maximum swelling and decreased the swelling rate. Swelling results showed increased AMPS (-) and MAPTAC (+) increased swelling ratio at low crosslink densities caused by coulombic repulsion allowing for PBS adsorption. Denser crosslinks decreases the maximum swelling ratio regardless of the amount of positive or negative monomer in the hydrogel. These results led to the conclusion that slower diffusion may affect the enzyme's ability to convert substrate into product at high crosslink densities. At low

crosslink densities, the rate-limiting factor is the process of enzyme conversion into substrate.

The fabricated ACR/BIS and ACR/PEGDA gels compared the degradation of hydrolysable crosslinker PEGDA with non-degradable BIS crosslinked gels and ACR/AMPS/PEGDA and ACR/MAPTAC/PEGDA gels compared the degradation positively charged gels with negatively charged gels. At high crosslink densities, PEGDA gels show lower swelling over time. The increased PEGDA density causes decreases in the swelling rate and makes it more difficult for solution to diffuse into the gel. A large number of these crosslinks must be degraded to increase the diffusion of degradation media into the gel. With fewer hydroxyl molecules reaching the hydrolysable PEGDA bonds, the degradation is slowed. Degradation results seen at 10 mole % crosslinked hydrogels containing 0-20 mole % MAPTAC monomer shows increased degradation rate with increased positive monomer content. Addition of AMPS (-) monomer agreed with this observation but had one anomaly to this trend seen in the 7 mole % crosslinked gels where the 20 mole % AMPS (-) gel showed a decreased degradation rate compared to 5, 10 and 15 mole % AMPS (-).

DMA studies of ACR/BIS gels showed increased LEM and SHM with increased crosslink density as expected. Gels in a fully swollen state showed reduced LEM and SHM as expected due to the increased PBS content. Interestingly, increasing the density of AMPS (-) or MAPTAC (+) monomer decreased the measured LEM. These variations are presumed to be an artifact of extra PBS content entering the gel due to the necessary experimental setup.

5.2 Biogel Characterization at Different Crosslink Densities

In order to make sure enzyme was not adsorbed to the surface and was adequately entrapped within the fabricated matrix confocal imaging was used to determine the enzyme dispersion within the gel. The results of confocal imaging studies determined that enzyme entrapment within the biogel was not uniform and that many more studies would be required to determine the relationship between crosslink density and any enzyme clustering. This behavior is expected to be due to the gel forcing the enzyme to cluster into small groups prior to complete polymerization, instead of being distributed evenly within the biogel.

This work demonstrated a repeatable, effective entrapment method that preserved enzyme activity within a favorable environment and resisted activity reduction due to a change in pH of the system. Lactase entrapped within ACR/BIS showed poor retention of initial and extended V_{\max} retention as compared to ACR/PEGDA hydrogel matrices. PEGDA acted to protect the enzyme from overall structural degradation and as PEGDA crosslink density increased between 5-10%, enzymatic retention increased. Crosslink densities of 15-40% decreased enzymatic retention due to steric hindrance of the enzyme and decreased diffusion of substrate to the active sites of the enzyme. This entrapment method showed marked improvement upon entrapment compared to alginate gels and shows promise for use in on-demand applications.

5.3 Biogel Characterization with Positive and Negative Monomer Moieties

Protection of the enzyme within hostile environments is of utmost importance in bringing this library of biogels into the hands of consumers for biosensor and

biomolecule product formation applications. AMPS (-) and MAPTAC (+) monomer moieties within the gel allow for increased stabilizing enzyme matrix interactions. High, 10 mole %, AMPS (-) monomer concentrations yielded the best storage and most reliable product molecule formation over a two day study. Enzyme activity as determined through the retention of the maximum velocity of ONPG conversion into ONP was tested in a BBS denaturation solution (pH 8). Most interesting was the positive correlation of AMPS (-) monomer concentration to V_{\max} retention when the biogels were tested with BBS. It is expected that the negative charges within the matrix effectively reduce the amount of negatively charged ions from being adsorbed, efficiently protecting the enzyme from this denaturation media.

5.4 Future Directions

Future directions of this work will create a more versatile biogel library by determining the relationship between enzyme activity and hydrophobic monomer moiety additions to the matrix construct. In order to complete this future aim it is necessary to characterize hydrophobic monomer effects on bulk matrix material properties through DMA, swelling and degradation experiments. After bulk properties are determined, enzymatic activity studies focusing on post-entrapment activity retention, two day cycling, and protection will be characterized.

Studies should continue to determine the distribution of enzyme within the fabricated biogels through fluorescent confocal microscopy. Clustering can be investigated by treating a dilute concentration of fluorescently labeled lactase with gluteraldehyde, creating enzyme clusters. These clusters can then be entrapped within the matrix to yield further understanding of the bright-spot analysis technique

attempted in this dissertation. After determining the correct analysis for protein clusters, the distribution of enzyme within the various biogels can be determined.

With rounded knowledge of charged and hydrophobic monomer moiety effects on the activity of the biogels and the distribution of enzyme within the biogels, the work will be optimized for a variety of desired enzymes. Preliminary optimization for new enzymes will begin with two basic elements; 1) using the known size of enzyme to relate to crosslink density, the smaller the enzyme the denser the crosslinks, and 2) using the enzyme's isoelectric pI, allowing to determine initial monomer moiety densities to increase enzyme stability and protection through enzyme/matrix interactions.

Optimizing the synthesized biogels for a different enzyme, using this library, will be proof of this method to allow for the easy and repeatable entrapment of any enzyme for the production of desired small molecules. Once efficacy of this method is proven, emphasis will move to on-demand applications. Multiple degradable crosslinkers will be tested to create a highly crosslinked biogel which, when the crosslinks are degraded, will become activated. Recruiting these innovations will lead to the creation of a generic method for the activation of any entrapped enzyme.

List of Acronyms

ACR:	Acrylamide
PEGDA:	Poly(ethylene glycol) diacrylate
BIS:	<i>N,N'</i> -methylenebisacrylamide
AMPS:	2-acrylamido-2-methyl-1-propanesulfonic acid sodium (negative)
MAPTAC:	[3-(methacryloylamino) propyl] trimethylammonium chloride (positive)
APS:	Ammonium persulfate
TEMED:	<i>N,N,N',N'</i> -tetramethylethylenediamine
PBS:	Phosphate buffered saline
ONPG:	Ortho-nitrophenyl- β -D-galactopyranoside
ONP:	Ortho-nitrophenol
DMA:	Dynamic mechanical analysis
BBS:	Borate buffer saline

Glossary

Biogel:	A biologically active hydrogel created by entrapping active enzyme within the polymer network during matrix formation.
E_a :	Activation energy, the minimum energy required to initiate a reaction.
Lactase:	i.e. β -galactosidase from <i>Kluyveromyces lactis</i> , a biologically active enzyme used in this work to degrade ONPG into ONP.
K_m :	Michaelis-Menton constant determined using Lineweaver-Burke plot, an indication of the enzyme pocket's binding efficiency
V_{max} :	The maximum velocity of conversion determined using Lineweaver-Burke plots

Bibliography

1. Lebiedzinska M, Szabadkai G, Jones AWE, Duszynski J, Wieckowski MR. Interactions between the endoplasmic reticulum, mitochondria, plasma membrane and other subcellular organelles. *International Journal of Biochemistry & Cell Biology*. 2009 Oct;41(10):1805-16.
2. Rybicka KK. Glycosomes - The organelles of glycogen metabolism. *Tissue & Cell*. 1996 Jun;28(3):253-65.
3. Romani AMP. Cellular magnesium homeostasis. *Archives of Biochemistry and Biophysics*. 2011 Aug 1;512(1):1-23.
4. Garcia-Viloca M, Gao J, Karplus M, Truhlar DG. How enzymes work: Analysis by modern rate theory and computer simulations. *Science*. 2004 Jan 9;303(5655):186-95.
5. Hult K, Berglund P. Engineered enzymes for improved organic synthesis. *Current Opinion in Biotechnology*. 2003 Aug;14(4):395-400.
6. Konig PM, Roth R, Dietrich S. Lock and key model system. *Epl*. 2008 Dec;84(6):-.
7. Odriozola G, Jimenez-Angeles F, Lozada-Cassou M. Entropy driven key-lock assembly. *Journal of Chemical Physics*. 2008 Sep 21;129(11):-.
8. Iyer PV, Ananthanarayan L. Enzyme stability and stabilization - Aqueous and non-aqueous environment. *Process Biochemistry*. 2008 Oct;43(10):1019-32.
9. Alonso N, Lopez-Gallego F, Betancor L, Hidalgo A, Mateo C, Guisan JM, et al. Immobilization and stabilization of glutaryl acylase on aminated sephabeads

supports by the glutaraldehyde crosslinking method. J Mol Catal B-Enzym. 2005 Aug 1;35(1-3):57-61.

10. Bolivar JM, Cava F, Mateo C, Rocha-Martin J, Guisan JM, Berenguer J, et al. Immobilization-stabilization of a new recombinant glutamate dehydrogenase from *Thermus thermophilus*. Applied Microbiology and Biotechnology. 2008 Aug;80(1):49-58.

11. Eijssink VGH, Gaseidnes S, Borchert TV, van den Burg B. Directed evolution of enzyme stability. Biomolecular Engineering. 2005 Jun;22(1-3):21-30.

12. Rao SV, Anderson KW, Bachas LG. Oriented immobilization of proteins. Mikrochimica Acta. 1998;128(3-4):127-43.

13. Xiao L, Honig B. Electrostatic contributions to the stability of hyperthermophilic proteins. Journal of Molecular Biology. 1999 Jun 25;289(5):1435-44.

14. Tannock GW, Ghazally S, Walter J, Loach D, Brooks H, Cook G, et al. Ecological behavior of *Lactobacillus reuteri* 100-23 is affected by mutation of the luxS gene. Appl Environ Microb. 2005 Dec;71(12):8419-25.

15. Vilchez R, Lemme A, Thiel V, Schulz S, Sztajer H, Wagner-Dobler I. Analysing traces of autoinducer-2 requires standardization of the *Vibrio harveyi* bioassay. Anal Bioanal Chem. 2007 Jan;387(2):489-96.

16. Sperandio V, Torres AG, Jarvis B, Nataro JP, Kaper JB. Bacteria-host communication: The language of hormones. P Natl Acad Sci USA. 2003 Jul 22;100(15):8951-6.

17. Sperandio V, Torres AG, Jarvis B, Nataro JP, Kaper JB. Bacteria-host communication: the language of hormones. *Proc Natl Acad Sci U S A*. 2003 Jul 22;100(15):8951-6.
18. Wagner C, El Omari M, Konig GM. Biohalogenation: Nature's Way to Synthesize Halogenated Metabolites. *J Nat Prod*. 2009 Mar;72(3):540-53.
19. Dean JLE, Colfen H, Harding SE, Rice DW, Engel PC. Alteration of the quaternary structure of glutamate dehydrogenase from *Clostridium symbiosum* by a single mutation distant from the subunit interfaces. *European Biophysics Journal with Biophysics Letters*. 1997;25(5-6):417-22.
20. Marsac Y CJ, Olschewski D, Alexandrov K, and Becker CFW. Site-Specific Attachment of Polyethylene Glycol-like Oligomers to Proteins and Peptides. *Bioconjugate Chem*. 2006;17:1492-8.
21. Santagapita PR, Mazzobre MF, Buera MP. Formulation and Drying of Alginate Beads for Controlled Release and Stabilization of Invertase. *Biomacromolecules*. 2011 Sep;12(9):3147-55.
22. Mariangela Bellusci IF, Andrea Marinelli, Lucio D'Ilario, and Antonella Piozzi. Lipase Immobilization on Differently Functionalized Vinyl-Based Amphiphilic Polymers: Influence of Phase Segregation on the Enzyme Hydrolytic Activity. *Biomacromolecules*. 2012;13:805-13.
23. Elnashar MMM, Yassin MA, Kahil T. Novel thermally and mechanically stable hydrogel for enzyme immobilization of penicillin G acylase via covalent technique. *J Appl Polym Sci*. 2008 Sep 15;109(6):4105-11.

24. Gill I, Ballesteros A. Bioencapsulation within synthetic polymers (Part 2): non-sol-gel protein-polymer biocomposites. *Trends in Biotechnology*. 2000 Nov;18(11):469-79.
25. Gill I, Ballesteros A. Bioencapsulation within synthetic polymers (Part 1): sol-gel encapsulated biologicals. *Trends in Biotechnology*. 2000 Jul;18(7):282-96.
26. Gupta R, Chaudhury NK. Entrapment of biomolecules in sol-gel matrix for applications in biosensors: Problems and future prospects. *Biosensors & Bioelectronics*. 2007 May 15;22(11):2387-99.
27. Mateo C, Fernandez-Lorente G, Abian O, Fernandez-Lafuente R, Guisan JM. Multifunctional epoxy supports: A new tool to improve the covalent immobilization of proteins. The promotion of physical adsorptions of proteins on the supports before their covalent linkage. *Biomacromolecules*. 2000 Win;1(4):739-45.
28. Wang QG, Yang ZM, Gao Y, Ge WW, Wang L, Xu B. Enzymatic hydrogelation to immobilize an enzyme for high activity and stability. *Soft Matter*. 2008;4(3):550-3.
29. Peppas NA, Merrill EW. Poly(vinyl-Alcohol) Hydrogels - Reinforcement of Radiation-Crosslinked Networks by Crystallization. *Journal of Polymer Science Part a-Polymer Chemistry*. 1976;14(2):441-57.
30. Alexander RS, Nair SK, Christianson DW. Engineering the Hydrophobic Pocket of Carbonic Anhydrase-II. *Biochemistry*. 1991 Nov 19;30(46):11064-72.
31. Janiak DS, Ayyub OB, Kofinas P. Effects of charge density on the recognition properties of molecularly imprinted polyampholyte hydrogels. *Polymer*. 2010 Feb 5;51(3):665-70.

32. Janiak DS, Ayyub OB, Kofinas P. Effects of Charge Density on the Recognition Properties of Molecularly Imprinted Polymeric Hydrogels. *Macromolecules*. 2009 Mar 10;42(5):1703-9.
33. Peppas NA, Hilt JZ, Khademhosseini A, Langer R. Hydrogels in biology and medicine: From molecular principles to bionanotechnology. *Adv Mater*. 2006 Jun 6;18(11):1345-60.
34. Tasdelen B, Kayaman-Apohan N, Guven O, Baysal BM. Swelling and diffusion studies of poly(N-isopropylacrylamide/itaconic acid) copolymeric hydrogels in water and aqueous solutions of drugs. *J Appl Polym Sci*. 2004 Jan 15;91(2):911-5.
35. Lee KY, Rowley JA, Eiselt P, Moy EM, Bouhadir KH, Mooney DJ. Controlling mechanical and swelling properties of alginate hydrogels independently by cross-linker type and cross-linking density. *Macromolecules*. 2000 May 30;33(11):4291-4.
36. Sadeghi M, Ghasemi N, Soleimani F. Optimization of Synthetic Conditions of a Novel Graft Copolymer Based on Alginate. *European Journal of Scientific Research*. 2011;64(4):587-97.
37. Kuoa C, Ma P. Ionically crosslinked alginate hydrogels as scaffolds for tissue engineering: Part 1. Structure, gelation rate and mechanical properties. *Biomaterials*. 2001;22(6):511-21.